

Compositional and orientational ordering in rod-coil diblock copolymer melts

Manuel Reenders* and Gerrit ten Brinke

*Department of Polymer Chemistry and Materials Science Center,
University of Groningen, Nijenborgh 4, 9747 AG Groningen, The Netherlands*

(October 30, 2018)

Abstract

The phase behavior of a melt of monodisperse rod-coil diblocks is studied. We derive a Landau free energy functional for both a compositional and a nematic order parameter. The excluded volume interaction between the rod blocks is modeled by an attractive Maier-Saupe interaction. The incompatibility between rod- and coil blocks is modeled by the usual Flory-Huggins interaction. For a large volume fraction of the rods, a transition from isotropic to nematic to smectic C is observed upon decreasing the temperature, whereas for small rod volume fraction, spherical, hexagonal, and lamellar structures prevail. In the smectic C phase, the rod orientation angle with respect to the lamellar normal increases rapidly from 35 to 40° close to the nematic/smectic-C phase boundary to values between 45 and 55° .

I. INTRODUCTION

Due to chemical incompatibility flexible AB diblocks are known to phase separate on a microscopic scale characterized by the radius of gyration of the blocks. The morphology of the microphases in the melt is successfully described in various approaches, which treat the AB diblocks as Gaussian chains and the incompatibility by a Flory-Huggins interaction [1–4]. Rod-coil diblock copolymers are a special class of AB diblock copolymers. Besides the usual incompatibility between distinct blocks, the liquid crystalline behavior of the stiff blocks can have a profound effect on the phase behavior. The combination of phase separation and orientational ordering gives rise to a wealth of different phases. In this paper a theoretical description of both phase separation and orientational ordering is developed.

In experiments on various rod-coil or liquid crystalline polymeric systems interesting phase behavior and micro-structures are observed [5–14]. Linear rod-coil multi-block oligomers can have orientationally ordered lamellar, hexagonal, spherical (bcc), and bicontinuous cubic liquid crystalline structures when the rod volume fraction is less than the coil

*m.reenders@chem.rug.nl

fraction [5–8]. Schneider *et al.* [9] reported results on a particular rod-coil diblock copolymer melt in which microphase separation occurs for higher temperatures than the liquid-crystalline order; although at high temperatures the microphase is bcc or gyroid, whenever anisotropic orientational order starts to play a role, the lamellar or smectic phase appears. One of the most striking features is the appearance of smectic C phases, and so-called zig-zag and arrowhead phases [10,11] for intermediate rod volume fractions.

The theoretical description of the phase behavior of rod-coil diblock copolymers requires the introduction of a compositional (density) order parameter and a (anisotropic) orientational order parameter or nematic order parameter. In the work of Holyst and Schick [15], the interactions and the excluded volume effects such as the steric repulsion between the rod blocks are treated in an approximate manner via the Flory-Huggins interaction, Maier-Saupe interaction, and the incompressibility constraint. The stiff part of the diblocks can be modeled by rigid rods [15], wormlike chains [16] or freely jointed rods [17], having a Maier-Saupe interaction [18]. The isotropic-nematic transition in various polymer systems was studied in a number of papers [16,19–21]. Using self-consistent field theory, the interplay between phase separation and liquid crystalline order has been studied ignoring morphologies other than lamellar [22,23]. Gurovich found that copolymer melts can order in four distinct ways under the influence of external ordering fields (*e.g.*, electric fields) close to the spinodal point [24].

For large rod volume fractions, the smectic behavior of layered rod-coil diblock copolymers in the strong segregation limit was studied [25–27,23]. For small rod volume fractions, so-called hockey puck phases might appear in the strong segregation region [28] or whenever phase separation occurs prior to nematic ordering [29]. Recently, a two-dimensional dynamic mean field model using the Maier-Saupe interaction was employed for a melt of semiflexible polymers [21]. Also the time evolution of morphology formation was studied in two dimensions for liquid-crystal/polymer mixtures showing a large influence of nematic ordering on phase separation [30]. Moreover, in two dimensions, the phase behavior of rod-coil diblock copolymer melts was obtained using a self-consistent field lattice model [31]. Interestingly, evidence for the existence of metastable zigzag structures which have been observed in experiments [10,11], was found [31].

In this paper, along the lines of Holyst and Schick [15] and Singh *et al.* [17], a monodisperse incompressible rod-coil diblock copolymer melt is studied with both a Flory-Huggins interaction and a Maier-Saupe interaction. The Maier-Saupe interaction models the steric repulsion between the rods, and henceforth favors alignment. Special attention is paid for the interplay between nematic ordering and microphase separation. One of the main questions addressed is: “How does the nematic ordering affect the microphase separation?” The Landau free energy is calculated up to the fourth order in two order parameters in the weak segregation limit. A density order parameter describes the tendency to microphase separation, whereas a nematic order parameter describes anisotropic alignment of rods in the melt. For blends, the free energy up to fourth order was already obtained by Liu and Fredrickson [16]. Perhaps another way of addressing the current issue is using the density functional formalism, *e.g.*, see the paper by Fukuda and Yokoyama [32] and references therein.

The setup of the present paper is as follows. In the next section a description of the partition function describing the rod-coil diblock melt is given, followed by an introduction into the Landau mean field expansion. Subsequently, the free energy expansion up to sec-

ond order is briefly reviewed, illustrating the instability of the isotropic phase with respect to nematic ordering and microphase separation. Then, the actual Landau free energy up to the fourth order is derived in the so called first harmonics approximation (FHA). The minimization of the free energy and the corresponding phase diagrams are discussed. In Appendix A the second order Landau coefficient or inverse “scattering matrix” is computed. Finally in Appendix B and C the pertinent three- and four-point single chain correlation functions and vertices are given.

II. THE MODEL

We consider an incompressible melt of n monodisperse rod-coil diblocks in volume V . The flexible (coil) part of the diblock is modeled by a Gaussian chain, and the rigid part by a “thin” rod. Each diblock molecule consists of N segments of which $N_C = f_C N$ are coil segments and $N_R = f_R N$ are rod segments, with $f_R = (1 - f_C)$. Thus, the volume fraction of the coil part is given by $f_C = N_C/N$. We keep the total density constant, $\rho_0 = nN/V$. The characteristic length scale of the coil block is given by the radius of gyration, $R_g = b\sqrt{N_C/6}$, with b the statistical coil segment length scale. The length of the rod is characterized by $\ell = N_R b'$, with b' the rod segment length. In this paper, we set $b = b' = 1$, thus $\rho_0 = nN/V = 1/b^3 = 1$.

The Hamiltonian for our melt contains two terms: one describing the standard Flory-Huggins repulsion between the rod and coil blocks and a second term describing orientational ordering of the rod blocks in the melt. The Hamiltonian for our model is

$$H_I = \chi \int d\vec{x} \rho_R(\vec{x}) \rho_C(\vec{x}) - \frac{\omega}{2} \int d\vec{x} S_R^{\mu\nu}(\vec{x}) S_R^{\mu\nu}(\vec{x}), \quad (\mu, \nu = 1, \dots, 3) \quad (1)$$

where ρ_C and ρ_R are the densities of the coil and the rod blocks, respectively, and $S_R^{\mu\nu}$ is the nematic order parameter tensor. The tensor $S_R^{\mu\nu}$ is symmetric and traceless. χ is the usual Flory-Huggins parameter. The second term in Eq. (1) is the Maier-Saupe interaction with the parameter ω . It effectively describes the excluded volume interaction between the rod blocks in the melt favoring their alignment.

The conformation of a diblock in the melt is given by the vector function $\vec{r}(\tau)$ describing the contour of the coil, the vector \vec{R} giving the position of the joint, and the unit vector \vec{u} describing the orientation of the rod, see Fig. 1. Then, the (single-chain) partition function of a rod-coil diblock in external fields is

$$Q[w_R, w_C, W^{\mu\nu}] = C \int \mathcal{D}\vec{r} d\vec{R} d\vec{u} \delta(\vec{r}(f_C) - \vec{R}) \delta(|\vec{u}| - 1) \\ \times \exp \left\{ -\frac{3}{2Nb^2} \int_0^{f_C} d\tau |\dot{\vec{r}}|^2 + \int w_R \hat{\rho}_R + \int w_C \hat{\rho}_C + \int W^{\mu\nu} \hat{S}_R^{\mu\nu} \right\}. \quad (2)$$

where $W^{\mu\nu}$ is an external tensor field which couples to the nematic-order operator. The normalization constant C is chosen such that $Q[0, 0, 0] = 1$. The density and orientational operators are

$$\hat{\rho}_R(\vec{x}) = \frac{f_R N}{\ell} \int_0^\ell ds \delta(\vec{x} - \vec{R} - s\vec{u}), \quad (3)$$

$$\hat{\rho}_C(\vec{x}) = N \int_0^{f_C} ds \delta(\vec{x} - \vec{r}(s)), \quad (4)$$

$$\hat{S}_R^{\mu\nu}(\vec{x}) = \frac{f_R N}{\ell} \int_0^\ell ds \delta(\vec{x} - \vec{R} - s\vec{u}) \left[u^\mu u^\nu - \frac{1}{3} \delta^{\mu\nu} u^2 \right]. \quad (5)$$

From Eqs. (2)-(5) all single chain correlation functions can be obtained by differentiating Q with respect to the external fields.

The partition function of the whole incompressible melt can be described by

$$\begin{aligned} \mathcal{Z} = & \left\{ \prod_{m=1}^n \int \mathcal{D}\vec{r}_m d\vec{R}_m d\vec{u}_m \mathcal{P}[\{\vec{r}_m, \vec{R}_m, \vec{u}_m\}] \right\} \delta(1 - \hat{\rho}_R(\vec{x}) - \hat{\rho}_C(\vec{x})) \\ & \times \exp \left\{ -\chi \int d\vec{x} \hat{\rho}_R(\vec{x}) \hat{\rho}_C(\vec{x}) + \frac{\omega}{2} \int d\vec{x} \hat{S}_R^{\mu\nu}(\vec{x}) \hat{S}_R^{\mu\nu}(\vec{x}) \right\}, \end{aligned} \quad (6)$$

where

$$\mathcal{P}[\{\vec{r}_m, \vec{R}_m, \vec{u}_m\}] = C \delta(\vec{r}_m(f_C) - \vec{R}_m) \delta(|\vec{u}_m| - 1) \exp \left\{ -\frac{3}{2Nb^2} \int_0^{f_C} d\tau |\dot{\vec{r}}_m|^2 \right\}. \quad (7)$$

After a number of Legendre transformations, we obtain

$$\begin{aligned} \mathcal{Z} \propto & \int \mathcal{D}\psi_R \mathcal{D}\psi_C \mathcal{D}S_R^{\mu\nu} \mathcal{D}J_R \mathcal{D}J_C \mathcal{D}J^{\mu\nu} \delta(\psi_R + \psi_C) \\ & \times \delta \left(\int \psi_R \right) \delta \left(\int \psi_C \right) \delta \left(\int J_R \right) \delta \left(\int J_C \right) \\ & \times \exp \left\{ -\chi \int \psi_R \psi_C + \frac{\omega}{2} \int S_R^{\mu\nu} S_R^{\mu\nu} \right\} \\ & \times \exp \left\{ -\int J_R \psi_R - \int J_C \psi_C - \int J^{\mu\nu} S_R^{\mu\nu} - G[J_R, J_C, J^{\mu\nu}] \right\}, \end{aligned} \quad (8)$$

where

$$G[J_R, J_C, J^{\mu\nu}] = -n \ln Q[J_R, J_C, J^{\mu\nu}], \quad (9)$$

and where we have introduced the fields

$$\psi_C(\vec{x}) = \rho_C(\vec{x}) - f_C, \quad \psi_R(\vec{x}) = \rho_R(\vec{x}) - f_R. \quad (10)$$

Making use of the above definition of G , the Landau mean field free energy can be obtained as an expansion in powers of the concentration profiles ψ_R , ψ_C and the nematic order parameter $S_R^{\mu\nu}$.

III. THE LANDAU MEAN-FIELD FREE ENERGY

We can write the ‘‘entropic’’ and ‘‘interaction’’ parts, respectively, of Eq. (8) as follows:

$$\exp \{-F_I[\phi]\} \equiv \exp \left\{ -I_{\alpha\beta} \int \phi_\alpha \phi_\beta \right\}, \quad (11)$$

$$\exp \{-F_S[\phi]\} \equiv \int \mathcal{D}J \exp \left\{ -\int J_\alpha \phi_\alpha - G[J] \right\}, \quad (12)$$

with the shorthand notation,

$$\phi_\alpha = (\psi_R, \psi_C, S_R^{\mu\nu}), \quad (13)$$

$$J_\alpha = (J_R, J_C, J^{\mu\nu}), \quad (14)$$

$$\hat{\rho}_\alpha = (\hat{\rho}_R, \hat{\rho}_C, \hat{S}_R^{\mu\nu}). \quad (15)$$

Thus the Greek index $\alpha = R, C, S$. So that

$$\mathcal{Z} = \exp \{-\mathcal{F}\} \propto \int \mathcal{D}\phi \exp \{-F[\phi]\}, \quad F = F_I + F_S. \quad (16)$$

The entropic part of the Landau free energy reads

$$\begin{aligned} \frac{NF_S}{V} &= \frac{1}{2!V^2} \sum_{k_1} \phi_\alpha(k_1) \phi_\beta(-k_1) \Gamma_{\alpha\beta}^{(2)}(k_1) \\ &+ \frac{1}{3!V^3} \sum_{k_1} \sum_{k_2} \phi_\alpha(k_1) \phi_\beta(k_2) \phi_\gamma(-k_1 - k_2) \Gamma_{\alpha\beta\gamma}^{(3)}(k_1, k_2) \\ &+ \frac{1}{4!V^4} \sum_{k_1} \sum_{k_2} \sum_{k_3} \phi_\alpha(k_1) \phi_\beta(k_2) \phi_\gamma(k_3) \phi_\delta(-k_1 - k_2 - k_3) \\ &\times \Gamma_{\alpha\beta\gamma\delta}^{(4)}(k_1, k_2, k_3). \end{aligned} \quad (17)$$

The vertices Γ are

$$\Gamma_{\alpha\beta}^{(2)}(k_1) = [W_{\alpha\beta}^{(2)}(k_1)]^{-1}, \quad (18)$$

$$\Gamma_{\alpha\beta\gamma}^{(3)}(k_1, k_2) = -\Gamma_{\alpha\alpha'}^{(2)}(k_1) \Gamma_{\beta\beta'}^{(2)}(k_2) \Gamma_{\gamma\gamma'}^{(2)}(-k_1 - k_2) W_{\alpha'\beta'\gamma'}^{(3)}(k_1, k_2), \quad (19)$$

and

$$\begin{aligned} \Gamma_{\alpha\beta\gamma\delta}^{(4)}(k_1, k_2, k_3) &= -\Gamma_{\alpha\alpha'}^{(2)}(k_1) \Gamma_{\beta\beta'}^{(2)}(k_2) \Gamma_{\gamma\gamma'}^{(2)}(k_3) \Gamma_{\delta\delta'}^{(2)}(-k_1 - k_2 - k_3) \\ &\times \left[W_{\alpha'\beta'\gamma'\delta'}^{(4)}(k_1, k_2, k_3) - \delta_K(k_1 + k_2) W_{\alpha\beta}^{(2)}(k_1) W_{\gamma\delta}^{(2)}(k_3) \right. \\ &- \delta_K(k_1 + k_3) W_{\alpha\gamma}^{(2)}(k_1) W_{\beta\delta}^{(2)}(k_2) - \delta_K(k_2 + k_3) W_{\alpha\delta}^{(2)}(k_1) W_{\beta\gamma}^{(2)}(k_2) \\ &- W_{\alpha'\beta'\mu}^{(3)}(k_1, k_2) \Gamma_{\mu\nu}^{(2)}(-k_1 - k_2) W_{\nu\gamma'\delta'}^{(3)}(k_1 + k_2, k_3) \\ &- W_{\alpha'\gamma'\mu}^{(3)}(k_1, k_3) \Gamma_{\mu\nu}^{(2)}(-k_1 - k_3) W_{\nu\beta'\delta'}^{(3)}(k_1 + k_3, k_2) \\ &\left. - W_{\alpha'\delta'\mu}^{(3)}(k_1, -k_1 - k_2 - k_3) \Gamma_{\mu\nu}^{(2)}(k_2 + k_3) W_{\nu\gamma'\beta'}^{(3)}(-k_2 - k_3, k_3) \right]. \end{aligned} \quad (20)$$

The functions $W^{(n)}$ are the single chain correlation functions

$$W_{\alpha_1\alpha_2\cdots\alpha_n}^{(n)}(k_1, k_2, \cdots, k_{n-1}) \equiv N^{-n} \langle \hat{\rho}_{\alpha_1}(k_1) \hat{\rho}_{\alpha_2}(k_2) \cdots \hat{\rho}_{\alpha_n}(-\sum_{i=1}^{n-1} k_i) \rangle_0, \quad (21)$$

where the average $\langle \cdots \rangle_0$ is defined as

$$\langle \mathcal{F}[\{\vec{r}, \vec{R}, \vec{u}\}] \rangle_0 \equiv \int \mathcal{D}\vec{r} d\vec{R} d\vec{u} \mathcal{P}[\{\vec{r}, \vec{R}, \vec{u}\}] \mathcal{F}[\{\vec{r}, \vec{R}, \vec{u}\}], \quad (22)$$

where \mathcal{P} is given by Eq. (7).

IV. THE SPINODAL

First, we consider the Landau expansion up to second order in the density and nematic order parameters, to analyze the instability of the isotropic phase with respect to microphase separation and nematic ordering. Therefore, following the approach of Holyst and Schick [15] and Singh *et al.* [17], we consider the free energy

$$\mathcal{F}[\psi, S] = \frac{1}{2} \sum_{\vec{q}} (\psi(-\vec{q}), S(-\vec{q})) \Gamma^{(2)}(\vec{q}) \begin{pmatrix} \psi(\vec{q}) \\ S(\vec{q}) \end{pmatrix}, \quad (23)$$

where $\Gamma^{(2)}$ is a 2×2 “scattering matrix”. This matrix $\Gamma^{(2)}$ can be obtained from the matrix Γ given in Eq. (A14) in Appendix A;

$$\Gamma^{(2)} = \begin{pmatrix} h_{RR} + h_{CC} - 2h_{RC} - 2N\chi & 2(h_{RS} - h_{CS})/3 \\ 2(h_{RS} - h_{CS})/3 & \bar{h}_{SS} - 2N\omega/3 \end{pmatrix}, \quad (24)$$

where

$$\bar{h}_{SS} = \sum_{i=1}^3 h_{SSi} \left(\frac{q^\mu q^\nu}{q^2} - \frac{\delta^{\mu\nu}}{3} \right) \left(\frac{q^\rho q^\sigma}{q^2} - \frac{\delta^{\rho\sigma}}{3} \right) T_i^{\mu\nu\rho\sigma}(q), \quad (25)$$

see Appendix A. For the nematic order tensor $S_R^{\mu\nu}$ we have taken the Ansatz

$$S_R^{\mu\nu}(\vec{q}) = S(q) \left(\frac{q^\mu q^\nu}{q^2} - \frac{\delta^{\mu\nu}}{3} \right), \quad (26)$$

where S is a scalar function. The nematic ordering is taken parallel to the wave vector \vec{q} .

The “scattering matrix” $\Gamma^{(2)}$ depends on \vec{q} , f_R , N and the ratio $r = \omega/\chi$. The spinodal is determined by the root of the determinant of $\Gamma^{(2)}$;

$$\det \Gamma^{(2)} = 0 \quad \implies \quad \chi(\vec{q}, f_R, N, r). \quad (27)$$

The real spinodal is given by the global minimum of χ (*i.e.*, the highest T) with respect to \vec{q} . Whenever one of the eigenvalues (or both of them) of $\Gamma^{(2)}$ becomes negative, the isotropic phase becomes unstable. The onset of the nematically ordered phase is given by the minimum of the root χ at wave vector $q = 0$. The onset of microphase separation is given by the minimum of the root χ at some nonzero $q = q^*$, which gives the inverse characteristic length scale of the microphase. The minimum at $q = 0$ for nematic ordering gives rise to a global nematic order parameter $S(\vec{q}) \rightarrow S$. All this is discussed in detail by Singh *et al.* [17], although for slightly different microscopic models. The situation where spinodal instabilities with respect to two distinct wave vectors occur resembles the situation encountered in comb-coil diblock copolymers [33,34].

V. THE FIRST HARMONICS APPROXIMATION

In the previous section, we pointed out that the instability of the isotropic phase with respect to nematic fluctuations gives rise to a global nematic ordering. The density order

parameters are constrained; the volume integral of ψ_C and ψ_R should vanish. Therefore, the Fourier components $\psi_C(p)$ and $\psi_R(p)$ can only give contributions for nonzero p . The nematic order parameter is not constrained, and it predominantly describes global ordering corresponding to the zero mode $p = 0$ in Fourier space.

The Landau free energy given in Eq. (17) is not solvable as it is. A way to solve the minimization condition for Eq. (17) is to expand the order parameters in harmonics representing certain discrete symmetries. Therefore, we shall adopt the first harmonics approximation (FHA) for the density order parameter $\psi = \psi_R = -\psi_C$, *i.e.*, we take in momentum space

$$\psi(\vec{k}) \simeq \frac{\psi}{\sqrt{n_S}} \sum_{\vec{Q} \in H_S} E_\phi(\vec{Q}) \delta_K(\vec{Q} - \vec{k}), \quad |\vec{Q}| = q^*, \quad (28)$$

with q^* the radius of the first harmonics sphere, and where $E_\phi(\vec{Q})$ is a phase factor and H_S is the set of wave vectors \vec{Q} with radius $|\vec{Q}| = q^*$ describing a particular discrete symmetry S of the structure. The number n_S is half the number of vectors in H_S . For the lamellar morphology $n_{lam} = 1$, for hexagonal $n_{hex} = 3$, for bcc $n_{bcc} = 6$. Moreover, the phase factor $E_\phi(\vec{Q}) = 1$ for the basic morphologies of interest. Clearly, the FHA restricts the microphase morphologies to morphologies which can be described by a single amplitude or order parameter ψ . Especially the nematic ordering could give rise to more complex morphologies which require more than one amplitude. To keep the analysis manageable, morphologies, which would require more than one amplitude, are not considered in this paper.

As explained in the previous section, we can assume that the nematic ordering is global and thus described by a space independent order parameter proportional to the nematic director $\eta^\mu \eta^\nu - \delta^{\mu\nu}/3$. Thus the Ansatz for $S^{\mu\nu}$ is

$$S^{\mu\nu}(\vec{k}) \simeq S \delta_K(\vec{k}) \left(\eta^\mu \eta^\nu - \frac{\delta^{\mu\nu}}{3} \right) = S \delta_K(\vec{k}) \mathcal{N}^{\mu\nu}, \quad (29)$$

$$\mathcal{N}^{\mu\nu} \equiv \left(\eta^\mu \eta^\nu - \frac{\delta^{\mu\nu}}{3} \right), \quad \mathcal{N}^{\mu\nu} \mathcal{N}^{\mu\nu} = \frac{2}{3}. \quad (30)$$

where S on right-hand side is the space independent order parameter, and $|\vec{\eta}| = 1$. With the Ansätze (28) and (29), the free energy can be expressed as

$$\begin{aligned} \mathcal{F}_S = & \left[c_{\psi\psi}^{(2)} - 2N\chi \right] \psi^2 + \left[c_{SS}^{(2)} - \frac{N\omega}{3} \right] S^2 + c_{\psi\psi\psi}^{(3)} \psi^3 + c_{\psi\psi S}^{(3)} \psi^2 S + c_{SSS}^{(3)} S^3 \\ & + c_{\psi\psi\psi\psi}^{(4)} \psi^4 + c_{\psi\psi\psi S}^{(4)} \psi^3 S + c_{\psi\psi SS}^{(4)} \psi^2 S^2 + c_{SSSS}^{(4)} S^4, \end{aligned} \quad (31)$$

where terms of the form ψS , ψS^2 and ψS^3 are absent in this approximation. The c coefficients are given in terms of γ functions, which are related to the Γ functions defined in Sec. III (see below):

$$c_{\psi\psi}^{(2)} = \frac{1}{2n_S} \sum_{Q_1} \sum_{Q_2} \delta_K(Q_1 + Q_2) \gamma_{\psi\psi}^{(2)}(Q_1), \quad (32)$$

$$c_{SS}^{(2)} = \frac{1}{2} \gamma_{SS}^{(2)}(0), \quad (33)$$

$$c_{\psi\psi\psi}^{(3)} = \frac{1}{3!n_S\sqrt{n_S}} \sum_{Q_1} \sum_{Q_2} \sum_{Q_3} \delta_K(Q_1 + Q_2 + Q_3) \gamma_{\psi\psi\psi}^{(3)}(Q_1, Q_2), \quad (34)$$

$$c_{\psi\psi S}^{(3)} = \frac{1}{2n_S} \sum_{Q_1} \sum_{Q_2} \delta_K(Q_1 + Q_2) \gamma_{\psi\psi S}^{(3)}(Q_1, Q_2), \quad (35)$$

$$c_{SSS}^{(3)} = \frac{1}{3!} \gamma_{SSS}^{(3)}(0, 0), \quad (36)$$

and

$$c_{\psi\psi\psi\psi}^{(4)} = \frac{1}{4!n_S^2} \sum_{Q_1} \sum_{Q_2} \sum_{Q_3} \sum_{Q_4} \delta_K(Q_1 + Q_2 + Q_3 + Q_4) \gamma_{\psi\psi\psi\psi}^{(4)}(Q_1, Q_2, Q_3), \quad (37)$$

$$c_{\psi\psi\psi S}^{(4)} = \frac{1}{3!n_S\sqrt{n_S}} \sum_{Q_1} \sum_{Q_2} \sum_{Q_3} \delta_K(Q_1 + Q_2 + Q_3) \gamma_{\psi\psi\psi S}^{(4)}(Q_1, Q_2, Q_3), \quad (38)$$

$$c_{\psi\psi SS}^{(4)} = \frac{1}{4n_S} \sum_{Q_1} \sum_{Q_2} \delta_K(Q_1 + Q_2) \gamma_{\psi\psi SS}^{(4)}(Q_1, Q_2, 0), \quad (39)$$

$$c_{SSSS}^{(4)} = \frac{1}{4!} \gamma_{SSSS}^{(4)}(0, 0, 0, 0). \quad (40)$$

In the above formulas the γ function are related to the Γ functions of Eq. (17) in the following way. The second order γ functions are

$$\gamma_{\psi\psi}^{(2)}(Q) \equiv \epsilon_a \epsilon_b \Gamma_{ab}^{(2)}(Q) = \Gamma_{RR}^{(2)}(Q) + \Gamma_{CC}^{(2)}(Q) - 2\Gamma_{RC}^{(2)}(Q), \quad (41)$$

$$\gamma_{SS}^{(2)}(0) \equiv \mathcal{N}^{\mu\nu} \mathcal{N}^{\rho\sigma} \Gamma_{SS}^{(2)\mu\nu\rho\sigma}(0) = \mathcal{N} \mathcal{N} \Gamma_{SS}^{(2)}(0), \quad (42)$$

with \mathcal{N} given in Eq. (30), and where $\psi_R = \epsilon_R \psi$, $\psi_C = \epsilon_C \psi$,

$$\epsilon_R = 1, \quad \epsilon_C = -1. \quad (43)$$

The third order γ functions are (with $|Q_1| = |Q_2| = |Q_1 + Q_2|$)

$$\gamma_{\psi\psi\psi}^{(3)}(Q_1, Q_2) \equiv \epsilon_a \epsilon_b \epsilon_c \Gamma_{abc}^{(3)}(Q_1, Q_2), \quad (44)$$

$$\gamma_{\psi\psi S}^{(3)}(Q_1, -Q_1) \equiv \epsilon_a \epsilon_b \mathcal{N} \Gamma_{abS}^{(3)}(Q_1, -Q_1), \quad (45)$$

$$\gamma_{SSS}^{(3)}(0, 0) \equiv \mathcal{N} \mathcal{N} \mathcal{N} \Gamma_{SSS}^{(3)}(0, 0). \quad (46)$$

Finally the fourth order γ functions are (with $|Q_1| = |Q_2| = |Q_3| = |Q_1 + Q_2 + Q_3|$)

$$\gamma_{\psi\psi\psi\psi}^{(4)}(Q_1, Q_2, Q_3) \equiv \epsilon_a \epsilon_b \epsilon_c \epsilon_d \Gamma_{abcd}^{(4)}(Q_1, Q_2, Q_3), \quad (47)$$

$$\gamma_{\psi\psi\psi S}^{(4)}(Q_1, Q_2, -Q_1 - Q_2) \equiv \epsilon_a \epsilon_b \epsilon_c \mathcal{N} \Gamma_{abcS}^{(4)}(Q_1, Q_2, -Q_1 - Q_2), \quad (48)$$

$$\gamma_{\psi\psi SS}^{(4)}(Q_1, -Q_1, 0) \equiv \epsilon_a \epsilon_b \mathcal{N} \mathcal{N} \Gamma_{abSS}^{(4)}(Q_1, -Q_1, 0), \quad (49)$$

$$\gamma_{SSSS}^{(4)}(0, 0, 0) \equiv \mathcal{N} \mathcal{N} \mathcal{N} \mathcal{N} \Gamma_{SSSS}^{(4)}(0, 0, 0). \quad (50)$$

The coefficients $c^{(2)}$, $c^{(3)}$, $c^{(4)}$ depend on N , f_R , q^* , ω/χ , χ and the symmetry-group (LAM, HEX, BCC). Moreover, the coefficients $c^{(3)}$ and $c^{(4)}$ also depend on the angle θ between the director η and the orientation of the lattice of the microphase symmetry. The characteristic wave vector q^* depends on the architecture, N and f_R .

VI. MINIMIZATION OF THE FREE ENERGY

Upon minimization of the free energy Eq. (31), with respect to the order parameters ψ and S and the angle θ , we shall distinguish between seven different phases. These phase are:

1. The isotropic phase (I): $\psi = 0, S = 0$

Microphases (M): $\psi \neq 0, S = 0$

2. Lamellar (LAM)
3. Hexagonal (HEX)
4. BCC (BCC)

5. Nematic phase (N): $\psi = 0, S \neq 0$

Smectic phases (S): $\psi \neq 0, S \neq 0$

6. Smectic A: $\theta = 0$
7. Smectic C: $0 < \theta \leq \pi/2$

The smectic phases A and C are defined as lamellar density fluctuating microphases with either a nematic director parallel to the lamellar director (A) or with a nonzero angle θ between them (C).

As mentioned previously we assume that temperature and architecture are the two dominant parameters to play with, and therefore, following the reasoning by Singh *et al.* [17], we assume that both χ and ω scale inversely with the temperature T . This means that for a fixed ratio $r = \omega/\chi$ and fixed N , we can draw the usual two-dimensional χN vs f “phase diagrams”.

Clearly, in this fourth order Landau expansion the order parameters ψ and S should be reasonably small, *e.g.*, $\psi, S \ll 1$. For the usual microphase separation this is the case close to the critical point. However, the isotropic-nematic transition is first order due to the presence of the third order term in S in Eq. (31). Therefore, we investigate first the “weakness” of the first order isotropic-nematic transition. Assuming that we are in the region of parameter space such that $\psi = 0$, we are left with the free energy

$$\mathcal{F}_S^{nem} = \left[c_{SS}^{(2)} - \frac{N\omega}{3} \right] S^2 + c_{SSS}^{(3)} S^3 + c_{SSSS}^{(4)} S^4, \quad (51)$$

where the coefficients are explicitly given in the appendix. The coefficients are

$$c_{SS}^{(2)} = \frac{5}{2f_R^2}, \quad c_{SSS}^{(3)} = -\frac{25}{21f_R^3}, \quad c_{SSSS}^{(4)} = \frac{425}{196f_R^4}. \quad (52)$$

The free energy (51) has a first order phase transition to a nematic phase when

$$\left[c_{SS}^{(2)} - \frac{N\omega}{3} \right] \leq \frac{[c_{SSS}^{(3)}]^2}{4c_{SSSS}^{(4)}} \implies N\omega_c = 3 \left\{ c_{SS}^{(2)} - \frac{[c_{SSS}^{(3)}]^2}{4c_{SSSS}^{(4)}} \right\} = \frac{1}{f_R^2} \left(\frac{715}{102} \right), \quad (53)$$

where ω_c is the binodal value.¹ The critical value of S is given by

$$S_c = -\frac{c_{SSS}^{(3)}}{2c_{SSSS}^{(4)}} = \frac{14}{51}f_R \leq \frac{14}{51} \approx 0.27. \quad (54)$$

This is a typical value for S_c for nematic liquids [35]. Thus for large rod fractions f_R , the nematic order parameter is close to $1/3$. It is well established that the Landau expansion for coil-coil AB diblocks is highly weakly first order even far from the critical point in the $N\chi$ - f plane. There, the critical value, ψ_c , for the order parameter ψ is at least one order of magnitude less than S_c (e.g., $\psi_c \simeq 1/30$).

Now, suppose that we are in a regime (coil rich) of parameter space where the nematic order parameter is zero ($S = 0$) and consider the minimization of Eq. (31) with respect to ψ . The free energy in this region reads

$$\mathcal{F}_S = [c_{\psi\psi}^{(2)} - 2N\chi] \psi^2 + c_{\psi\psi\psi}^{(3)} \psi^3 + c_{\psi\psi\psi\psi}^{(4)} \psi^4. \quad (55)$$

The q^* was already (and can still be) determined from the minimum of $c_{\psi\psi}^{(2)}$ with respect to $|Q|$. By definition this minimum is q^* . The spinodal is then given by the equation

$$2N\chi_s = c_{\psi\psi}^{(2)}. \quad (56)$$

In the FHA the free energy for a lamellar morphology corresponding to q^* is known [1] to be given by

$$\mathcal{F}_S^{lam} = [c_{\psi\psi}^{(2)lam} - 2N\chi] \psi_l^2 + c_{\psi\psi\psi\psi}^{(4)lam} \psi_l^4, \quad (57)$$

where (with $|Q| = q^*$)

$$c_{\psi\psi}^{(2)lam} = \frac{1}{2} \sum_{Q_1 \in lam} \sum_{Q_2 \in lam} \delta_K(Q_1 + Q_2) \gamma_{\psi\psi}^{(2)}(Q_1) = \gamma_{\psi\psi}^{(2)}, \quad (58)$$

$$c_{\psi\psi\psi\psi}^{(4)lam} = \frac{1}{4} \gamma_{\psi\psi\psi\psi}^{(4)}, \quad (59)$$

with $\gamma_{\psi\psi}^{(2)}$ and $\gamma_{\psi\psi\psi\psi}^{(4)}$ explicitly given in the appendix. The hexagonal and bcc morphologies have free energies:

$$\mathcal{F}_S^{hex} = [c_{\psi\psi}^{(2)hex} - 2N\chi] \psi_h^2 + c_{\psi\psi\psi}^{(3)hex} \psi_h^3 + c_{\psi\psi\psi\psi}^{(4)hex} \psi_h^4, \quad (60)$$

$$\mathcal{F}_S^{bcc} = [c_{\psi\psi}^{(2)bcc} - 2N\chi] \psi_b^2 + c_{\psi\psi\psi}^{(3)bcc} \psi_b^3 + c_{\psi\psi\psi\psi}^{(4)bcc} \psi_b^4, \quad (61)$$

with

$$c_{\psi\psi}^{(2)hex} = \gamma_{\psi\psi}^{(2)}, \quad c_{\psi\psi\psi}^{(3)hex} = \frac{2}{3\sqrt{3}} \gamma_{\psi\psi\psi}^{(3)}, \quad c_{\psi\psi\psi\psi}^{(4)hex} = \frac{1}{12} \gamma_{\psi\psi\psi\psi}^{(4)} + \frac{1}{3} \gamma_{\psi\psi\psi\psi}^{(4)}, \quad (62)$$

¹The value $\omega_s = 15/(2f_R^2)$ is the so-called spinodal value corresponding to the change of sign of the second order term.

respectively,

$$\begin{aligned}
c_{\psi\psi}^{(2)bcc} &= \gamma_{\psi\psi}^{(2)}, & c_{\psi\psi\psi}^{(3)bcc} &= \frac{4}{3\sqrt{6}}\gamma_{\psi\psi\psi}^{(3)}, \\
c_{\psi\psi\psi\psi}^{(4)bcc} &= \frac{1}{24}\gamma_{\psi\psi\psi\psi 1}^{(4)} + \frac{1}{3}\gamma_{\psi\psi\psi\psi 2}^{(4)} + \frac{1}{12}\gamma_{\psi\psi\psi\psi 3}^{(4)} + \frac{1}{6}\gamma_{\psi\psi\psi\psi 4}^{(4)}.
\end{aligned} \tag{63}$$

For fixed $N\chi$, r , f_R and N , it is then straightforward to find the morphology with lowest free energy.

The next step is to consider the region of the phase diagram where $\psi \ll S < 1$. In this case if the temperature is lowered first the isotropic to nematic transition is encountered meaning that the lowering of the free energy is primarily driven by the appearance of a nonzero value for S . When the temperature is decreased ($N\chi \uparrow$), the appearance of a microphase structure ($\psi \neq 0$) lowers the free energy further. In this particular case, the value of S is mainly determined by Eq. (51). The value of ψ then follows from the free energy part of Eq. (31),

$$\mathcal{F}_S^{mix} = [c_{\psi\psi}^{(2)} + c_{\psi\psi S}^{(3)}S + c_{\psi\psi SS}^{(4)}S^2 - 2N\chi] \psi^2 + [c_{\psi\psi\psi}^{(3)} + c_{\psi\psi\psi S}^{(4)}S] \psi^3 + c_{\psi\psi\psi\psi}^{(4)}\psi^4, \tag{64}$$

in which S should be considered as an external field. The total free energy being $\mathcal{F}_S = \mathcal{F}_S^{nem} + \mathcal{F}_S^{mix}$. In the above Eq. (64) the angle θ comes into play.

For instance, if the morphology is assumed to be lamellar, the coupling term $c_{\psi\psi S}^{(3)}$ can be written as

$$\begin{aligned}
c_{\psi\psi S}^{(3)lam} &= \frac{\gamma_{\psi\psi S}^{(3)}}{2n_{lam}} \sum_{Q \in lam} P_2(\hat{Q} \cdot \eta) = \frac{\gamma_{\psi\psi S}^{(3)}}{2} [P_2(\hat{Q} \cdot \eta) + P_2(-\hat{Q} \cdot \eta)] \\
&= P_2(\cos \theta) \gamma_{\psi\psi S}^{(3)},
\end{aligned} \tag{65}$$

with $\hat{Q} = \vec{Q}/q^*$, $\cos \theta = \hat{Q} \cdot \eta$. In case of a hexagonal morphology (with six lattice vectors \vec{Q}_i), we get

$$c_{\psi\psi S}^{(3)hex} = \frac{\gamma_{\psi\psi S}^{(3)}}{2n_{hex}} \sum_{Q \in hex} P_2(\hat{Q} \cdot \eta) = \frac{\gamma_{\psi\psi S}^{(3)}}{3} \sum_{i=1}^3 P_2(\hat{Q}_i \cdot \eta), \tag{66}$$

and for the bcc morphology

$$c_{\psi\psi S}^{(3)bcc} = \frac{\gamma_{\psi\psi S}^{(3)}}{2n_{bcc}} \sum_{Q \in bcc} P_2(\hat{Q} \cdot \eta) = \frac{\gamma_{\psi\psi S}^{(3)}}{6} \sum_{i=1}^6 P_2(\hat{Q}_i \cdot \eta), \tag{67}$$

The other coupling terms in Eq. (64) are decomposed as

$$\begin{aligned}
c_{\psi\psi SS}^{(4)sym} &= \frac{1}{4n_{sym}} \sum_{Q \in sym} [\gamma_{\psi\psi SS0}^{(4)} + \gamma_{\psi\psi SS1}^{(4)}P_2(\hat{Q} \cdot \eta) + \gamma_{\psi\psi SS2}^{(4)}P_2^2(\hat{Q} \cdot \eta)] \\
&= \frac{1}{2} [\gamma_{\psi\psi SS0}^{(4)} + \gamma_{\psi\psi SS1}^{(4)}A_{1sym}(\Omega) + \gamma_{\psi\psi SS2}^{(4)}A_{2sym}(\Omega)],
\end{aligned} \tag{68}$$

where *sym* stands for either one of three basic morphologies, and

$$A_{1sym}(\Omega) = \frac{1}{2n_{sym}} \sum_{Q \in sym} P_2(\hat{Q} \cdot \eta), \quad A_{2sym}(\Omega) = \frac{1}{2n_{sym}} \sum_{Q \in sym} P_2^2(\hat{Q} \cdot \eta), \quad (69)$$

with Ω the three dimensional space angle between the nematic vector $\vec{\eta}$ and the orientation vector of the lattice corresponding to the space symmetry group *sym*.

Subsequently, the free energy is written as

$$\mathcal{F}_S^{mix} = \alpha_1 \psi^2 - \alpha_2 \psi^3 + \alpha_3 \psi^4, \quad (70)$$

with

$$\alpha_1 = c_{\psi\psi}^{(2)} + c_{\psi\psi S}^{(3)} S + c_{\psi\psi SS}^{(4)} S^2 - 2N\chi, \quad (71)$$

$$\alpha_2 = - \left[c_{\psi\psi\psi}^{(3)} + c_{\psi\psi\psi S}^{(4)} S \right], \quad (72)$$

$$\alpha_3 = c_{\psi\psi\psi\psi}^{(4)}. \quad (73)$$

Then for the lamellar morphology (thus smectic), these coefficients can be expressed as

$$\begin{aligned} \alpha_1 &= -2N\chi + \beta_0(q^*) + \beta_1(q^*)P_2(\cos \theta) + \beta_2(q^*)P_2^2(\cos \theta), \\ \alpha_2 &= 0, \quad \alpha_3 = \frac{1}{4}\gamma_{\psi\psi\psi\psi 1}^{(4)}, \end{aligned} \quad (74)$$

where $\cos \theta = (\eta \cdot \vec{Q})/q^*$. The functions β_i are

$$\beta_0 = c_{\psi\psi}^{(2)} + \frac{1}{2}\gamma_{\psi\psi SS 0}^{(4)} S^2, \quad \beta_1 = \gamma_{\psi\psi S}^{(3)} S + \frac{1}{2}\gamma_{\psi\psi SS 1}^{(4)} S^2, \quad \beta_2 = \frac{1}{2}\gamma_{\psi\psi SS 2}^{(4)} S^2. \quad (75)$$

Now the minimum of \mathcal{F}_S^{mix} with respect to θ corresponds to the minimum of α_1 , since α_3 does not depend on θ . Since $\beta_1 < 0$ and $\beta_2 > 0$, the minimum of α_1 with respect to $\cos \theta$ is

$$\alpha_1 = -2N\chi + \beta_0 - \frac{\beta_1^2}{4\beta_2}, \quad (76)$$

with

$$\theta_{min} = \arccos \left(\sqrt{\frac{\beta_2 - \beta_1}{3\beta_2}} \right). \quad (77)$$

Numerically it turns out that $\gamma_{\psi\psi SS 2}^{(4)}$ is roughly one order of magnitude larger than $\gamma_{\psi\psi SS 1}^{(4)}$ and $\gamma_{\psi\psi SS 0}^{(4)}$ for a large range of volume fractions f_C . Since the nematic order parameter S is close to 1/3 or even larger (*e.g.*, see Eq. (54)), the consequence is that in general $\beta_2 \gg \beta_1$ and therefore the angle θ is close to

$$\theta_m \approx \arccos \sqrt{1/3} \approx 54^\circ. \quad (78)$$

Thus a smectic C phase with an angle of about 54° is obtained in the region of parameter space where nematic instabilities precede density fluctuations.

However, the above conclusion is premature unless the other two morphologies are considered. For these morphologies, besides the terms already given in Eqs. (66), (67), and (68), third order density terms are present and consequently the coupling term

$$c_{\psi\psi\psi Ssym}^{(4)} = \frac{1}{3!n_{sym}\sqrt{n_{sym}}} \sum_{Q_1 \in sym} \sum_{Q_2 \in sym} \gamma_{\psi\psi\psi S}^{(4)}(Q_1, Q_2, -Q_1 - Q_2), \quad (79)$$

plays a role. This term is written as

$$c_{\psi\psi\psi Shex}^{(4)} = \frac{2}{3\sqrt{3}} \sigma_{\psi\psi\psi S} \left[P_2(\hat{Q}_1 \cdot \eta) + P_2(\hat{Q}_2 \cdot \eta) + P_2(\hat{Q}_3 \cdot \eta) \right], \quad (80)$$

$$c_{\psi\psi\psi Sbcc}^{(4)} = \frac{4}{3\sqrt{6}} \sigma_{\psi\psi\psi S} \left[P_2(\hat{Q}_1 \cdot \eta) + P_2(\hat{Q}_2 \cdot \eta) + P_2(\hat{Q}_3 \cdot \eta) \right], \quad (81)$$

with $Q_3 = -Q_1 - Q_2$ and $\sigma_{\psi\psi\psi S}$ defined in Eq. (B78). The three vectors Q_i can be an arbitrary triangle in the vector space of the first harmonic sphere of the particular lattice symmetry group (HEX or BCC). However, by comparing numerically the free energies of the hexagonal and bcc morphology with nonzero S in the FHA, it turns out that the smectic C phase (thus lamellar) has the lowest free energy in this particular region of the parameter space.

In the coil rich region of the parameter space, it is possible to take a value for $r = \omega/\chi$ so that microphase separation occurs prior to nematic ordering, *i.e.*, with $S \ll \psi < 1$, on decreasing the temperature. In this case the order parameter ψ is mainly determined by Eq. (55). However, now the nematic order parameter S is driven by the field ψ which acts as an external field in the free energy part

$$\mathcal{F}_{mix} = \left[c_{\psi\psi S}^{(3)} \psi^2 + c_{\psi\psi\psi S}^{(4)} \psi^3 \right] S + \left[c_{SS}^{(2)} + c_{\psi\psi SS}^{(4)} \psi^2 - \frac{N\omega}{3} \right] S^2, \quad (82)$$

up to second order in S . We assume that the temperature is still above the binodal temperature (thus below $N\chi_c$) so that nematic ordering is purely density driven. Then

$$S_m \simeq - \frac{\left[c_{\psi\psi S}^{(3)} \psi^2 + c_{\psi\psi\psi S}^{(4)} \psi^3 \right]}{2 \left[c_{SS}^{(2)} - N\omega/3 \right]}. \quad (83)$$

For a large region of the phase diagram with the above constraint $S \ll \psi < 1$ it turns out that $S_m \ll S_c$ as given by Eq. (54). This concludes the analysis of the free energy, Eq. (31).

VII. THE PHASE DIAGRAM

In the previous section, we outlined the various steps in the minimization of the FHA free energy Eq. (31). This section is devoted to the actual computation and derivation of the phase diagrams. The first step in the process is to determine q^* . This wave vector q^* is given by the minimum of $\gamma_{\psi\psi}^{(2)}(q)$ of Eq. (B9) with respect to q . It is to be expected that the characteristic length scale for microphase separation is predominantly determined by the length $\ell = Nf_R$ of the rod part of the diblock. At least for large N and in the rod rich region this is to be expected, since the length scale of the rod part scales with N and that of the coil part with $N^{1/2}$. This means that the lowest q vector for the rod is much smaller than the lowest q vector of the coil part. The corresponding characteristic wave vector for the rod is $q^* = 2\pi/\ell = 2\pi/(Nf_R)$. In Fig. 2 the numerical value of q^* is depicted vs rod

fraction f_R and compared with the above-mentioned characteristic wave vector. From this figure it is clear that for a large region of f_R both q^* lie rather close together, supporting the view that the rod-length scale characterizes the microphases.

With q^* numerically computed as function of f_R , the higher point vertices $\gamma^{(3)}$ and $\gamma^{(4)}$ are determined, since these do not depend on χ and ω . Subsequently all c coefficients of the Landau free energy Eq. (31) are computed. Depending on the values of χ , r , N the phase diagram is constructed by minimizing the free energy with respect to ψ , S , and θ .

As pointed out in the previous section, when there is no Maier-Saupe interaction, there will be no accountable or notable value for the nematic order parameter S (*i.e.*, $S \ll 1/3$). The phase diagram for this situation where $\omega = 0$, *i.e.*, $r = 0$, is given in Figure 3 for $N = 40$. The asymmetry of the phase diagram with respect to the AB coil-coil diblock phase diagram (as first derived by Leibler [1]) is apparent. First of all, the critical point, which is given by the root of the $\gamma_{\psi\psi\psi}^{(3)}$ vertex, is shifted to the rod rich part. Beyond the critical point for even higher rod fraction the bcc phase is absent.

The coil rich part of the phase diagram is quite similar to an AB coil-coil diblock phase diagram with first the appearance of a bcc phase prior to hexagonal and lamellar phases. However, close to fraction $f_R \sim 0.4$ the bcc phase disappears at the triple point and for increasing χ only the hexagonal and lamellar phases are encountered. This is a result of the relative smallness of the ratio k ,

$$k \equiv \left(\frac{c_{\psi\psi\psi}^{(3)bcc}}{c_{\psi\psi\psi}^{(3)hex}} \right)^2 \frac{c_{\psi\psi\psi}^{(4)hex}}{c_{\psi\psi\psi}^{(4)bcc}}, \quad (84)$$

as compared to coil-coil diblock copolymers [1]. Whenever $k < 1$ the hexagonal phase is encountered first upon crossing the binodal curve from the isotropic phase. The triple point corresponds to $k = 1$.

The dependence on the ratio r is depicted in a series of figures, Fig. 3-Fig. 7. The isotropic-nematic phase boundary (PB) is roughly given by the spinodal curve

$$\chi_s = 15/(2r f_R^2), \quad (85)$$

see footnote in Sec. VI. Thus by increasing r , χ_s is lowered which appears as a shifting of the isotropic-nematic PB to the left. Whenever the nematic phase region “overlaps” with the microphase region a smectic C phase (lamellar) is favored over the bcc and hexagonal morphologies; nematic ordering favors lamellae. This results from the fact that, whenever a nonzero value for S appears, the second order coefficient α_1 in the Landau free energy for ψ (Eq. (70)) is considerable smaller for the lamellar phase than for the hexagonal phase, after minimization with respect to angles. Consequently, in the nematic phase region, the spinodal curve for the lamellar morphology (=smectic) lies below the binodal curves for the hexagonal and bcc morphologies. In the FHA the hexagonal and bcc morphologies are incompatible with nematic order, and a smectic (layered liquid crystalline) phase prevails.

Contour lines of the angle θ are depicted also in the figures. The dots denote “triple points”. The angle increases rapidly from 35 to 40° close to the nematic smectic-C phase boundary to values between 45 and 55°. This behavior is in agreement with the analysis in the previous section. In Fig. 7 the nematic phase region has completely overwhelmed the microphase region. Even in the coil rich region there is an isotropic-nematic transition. This

means that the microphases are absent all together and only the smectic C phase appears for lower temperatures.

If the overall length of the diblock is increased ($N \uparrow$) the critical point and the triple points will shift to the rod-rich part. However, qualitatively, the phase diagrams for fixed r but with different N are quite similar, as can be seen by comparing Figs. (5) and (8).

VIII. CONCLUDING REMARKS

In this paper, we studied an incompressible melt of rod-coil diblock copolymers. Both microphase separation and orientational ordering were investigated. We have derived a Landau expansion of the free energy of the melt up to fourth order in the two order parameters ψ and S , representing, respectively, compositional and nematic ordering. The compositional ordering or microphase separation was driven by the usual Flory-Huggins interaction, whereas the orientational ordering was driven by a Maier-Saupe interaction. Up to seven different phases of the melt could be distinguished as function of molecular architecture, temperature, and relative strength of the molecular interactions. The characteristic length scale for the microphases turned out to be roughly the length of the rod part of the diblock.

In comparison with the coil-coil (AB) diblocks, the phase diagram for rod-coil diblocks is quite asymmetric, with a critical point lying in the rod-rich region on the spinodal curve. Nevertheless, the spinodal curve for the rod-coil system is nearly symmetric. There is a complete absence of the spherical or bcc microphase in the rod-rich region, beyond the critical point. This is perhaps not so surprising, since it is hard to imagine spherical micelles of coil segments being embedded in a matrix of rods. The coil-rich region is more similar to a diblock, where the spherical microphase appears prior to hexagonal and lamellar structures when the temperature decreases. However, for intermediate rod-volume fractions, there is an interesting suppression of the bcc morphologies with respect to the hexagonal one. When crossing the binodal curve from the isotropic phase, the hexagonal phase appears instead of the bcc morphology. There is an isotropic-hexagonal-lamellar transition. Such a transition is rather uncommon for coil-coil (AB) diblocks. The general features of our phase diagram are in qualitative agreement with experiments on rod-coil systems with small and intermediate rod volume fractions [5–9]. Moreover, in these experimental papers, observations of bicontinuous cubic phases are reported. The description of these more complex phases is beyond the scope of the present paper, since it would require the introduction of an additional order parameter, namely, the amplitude of the second harmonics.

Most of the features mentioned above are governed by compositional ordering, which is most prominent in the coil-rich phase. However, different phase behavior is obtained when the orientational or nematic ordering is the driving force in the melt. Therefore, in the rod-region, with reasonable values for the Maier-Saupe interactions the main results are; the suppression of hexagonal and bcc structures in the rod-rich region of the phase diagram whenever nematic ordering occurs and the appearance of a smectic C phase in the rod-rich region, with a characteristic angle $45^\circ \leq \theta < 55^\circ$.

We have shown that when nematic phases appear prior to microphases upon decreasing the temperature, instead of the usual bcc or hexagonal morphologies a smectic C (lamellar) phase is obtained. Also we have found no evidence for smectic A phases in the rod rich region of the phase diagram. As was mentioned in the introduction, smectic C phases and

equivalent phases have been reported for experiments on rod-coil systems for intermediate to high rod volume fractions [10,11]. Moreover, the smectic angle θ is in quantitative agreement with the experimental observed values for θ , with $\theta \sim 45^\circ$.

At a first glance, the absence of a smectic A phase in the rod-rich region might seem to contradict earlier theoretical results [23,25–27], where the orientational alignment is chosen to be perfect (all rod segments are parallel, *i.e.*, $S \simeq 1$). However, one should realize that the present model describes a different limiting case of the rod-coil diblock copolymer melt. Clearly the free-energy expansion in order parameters breaks down, whenever one of the order parameters becomes too large, *e.g.*, when S approaches unity. Roughly speaking, the applicability of the Landau free energy is limited to the region in the $\chi N - f_R$ plane, where the spinodal curves for order parameters ψ and S intersect or lie reasonable close to one another. Although, it can be shown that the Maier-Saupe interaction is a valid approximation for the steric repulsion even when the alignment of rod-segments is nearly or completely parallel [18], the present model cannot really be compared to the other works [23,25–27] in great detail, due to the breakdown of the Landau expansion for the order parameter S .

ACKNOWLEDGMENTS

We would like to thank H. Angerman, I. Erukhimovich, S. Kuchanov, R. Nap, H. Slot, A. Subbotin, and A. Zvelindovsky for useful suggestions and stimulating discussions. This research was supported by SOFTLINK, a technology-related soft condensed matter research program of the Dutch organization for scientific research NWO.

APPENDIX A: THE SECOND ORDER VERTEX $\Gamma^{(2)}$

In this appendix, we compute the second order vertex $\Gamma^{(2)}$. The vertex $\Gamma^{(2)}$ is the inverse of the single chain correlation function $W^{(2)}$ as given by Eq. (18),

$$\Gamma_{\alpha\beta}^{(2)}(k_1) = [W_{\alpha\beta}^{(2)}(k_1)]^{-1}, \quad (\text{A1})$$

where the Greek index $\alpha = R, C, S$. We introduce the matrix

$$\mathbf{W}^{\mu\nu\rho\sigma} \equiv \begin{pmatrix} W_{RR}^{(2)} & W_{RC}^{(2)} & W_{RS}^{(2)\rho\sigma} \\ W_{CR}^{(2)} & W_{CC}^{(2)} & W_{CS}^{(2)\rho\sigma} \\ W_{SR}^{(2)\mu\nu} & W_{SC}^{(2)\mu\nu} & W_{SS}^{(2)\mu\nu\rho\sigma} \end{pmatrix}, \quad (\text{A2})$$

where

$$\begin{aligned} W_{RR}^{(2)}(p) &= N^{-2} \langle \hat{\rho}_R(\vec{p}) \hat{\rho}_R(-\vec{p}) \rangle_0 = \left(\frac{f_R}{\ell} \right)^2 \int_0^\ell \int_0^\ell ds ds' \langle e^{i(s-s')\vec{p}\cdot\vec{u}} \rangle_0 \\ &= f_R^2 K_{R1}^{(2)}(y) = g_{RR}(p), \end{aligned} \quad (\text{A3})$$

with $f_R = 1 - f_C$, and where the variable y is

$$y = N_R p. \quad (\text{A4})$$

The other functions are

$$W_{CC}^{(2)}(p) = f_C^2 K_{C1}^{(2)}(x) = g_{CC}(p), \quad (\text{A5})$$

$$W_{RC}^{(2)}(p) = W_{CR}^{(2)}(p) = f_C f_R K_C^{(1)}(x) K_R^{(1)}(y) = g_{RC}(p), \quad (\text{A6})$$

where the variable x is

$$x = N_C p^2 / 6, \quad (\text{A7})$$

and $K_{C1}^{(2)} = f_D$ is the Debye function and the K functions are defined in Appendix C. Furthermore, the two point single chain functions with one nematic tensor is

$$W_{RS}^{(2)\mu\nu}(p) = W_{SR}^{(2)\mu\nu}(p) = \left(\frac{p^\mu p^\nu}{p^2} - \frac{\delta^{\mu\nu}}{3} \right) f_R^2 K_{RS}^{(2)}(y) = \Delta^{\mu\nu} g_{RS}(p), \quad (\text{A8})$$

$$W_{CS}^{(2)\mu\nu}(p) = W_{SC}^{(2)\mu\nu}(p) = \left(\frac{p^\mu p^\nu}{p^2} - \frac{\delta^{\mu\nu}}{3} \right) f_R f_C K_C^{(1)}(x) K_{S0}^{(1)}(y) = \Delta^{\mu\nu} g_{CS}(p), \quad (\text{A9})$$

with $\Delta^{\mu\nu} = p^\mu p^\nu / p^2 - \delta^{\mu\nu} / 3$. Finally, the two point function with two nematic tensors is expressed as

$$W_{SS}^{(2)\mu\nu\rho\sigma}(p) = f_R^2 \sum_{i=1}^3 K_{Si}^{(2)}(y) \mathcal{T}_i^{\mu\nu\rho\sigma}(p) = \sum_{i=1}^3 \mathcal{T}_i^{\mu\nu\rho\sigma}(p) g_{SSi}(p), \quad (\text{A10})$$

where $g_{SSi} = f_R^2 K_{Si}^{(2)}(y)$, with $K_{Si}^{(2)}$ defined in Appendix C. The tensors are

$$\begin{aligned} \mathcal{T}_1^{\mu\nu\rho\sigma}(p) &\equiv \delta^{\nu\rho} \delta^{\mu\sigma} + \delta^{\nu\sigma} \delta^{\mu\rho} - \frac{14}{9} \delta^{\mu\nu} \delta^{\rho\sigma} \\ &\quad - 2\delta^{\nu\rho} \frac{p^\sigma p^\mu}{p^2} - 2\delta^{\nu\sigma} \frac{p^\rho p^\mu}{p^2} - 2\delta^{\mu\rho} \frac{p^\nu p^\sigma}{p^2} - 2\delta^{\mu\sigma} \frac{p^\rho p^\nu}{p^2} \\ &\quad + \frac{8}{3} \delta^{\mu\nu} \frac{p^\rho p^\sigma}{p^2} + \frac{8}{3} \delta^{\rho\sigma} \frac{p^\mu p^\nu}{p^2}, \end{aligned} \quad (\text{A11})$$

$$\begin{aligned} \mathcal{T}_2^{\mu\nu\rho\sigma}(p) &\equiv \delta^{\nu\rho} \frac{p^\sigma p^\mu}{p^2} + \delta^{\nu\sigma} \frac{p^\rho p^\mu}{p^2} + \delta^{\mu\rho} \frac{p^\sigma p^\nu}{p^2} + \delta^{\mu\sigma} \frac{p^\rho p^\nu}{p^2} \\ &\quad - \frac{4}{3} \delta^{\mu\nu} \frac{p^\rho p^\sigma}{p^2} - \frac{4}{3} \delta^{\sigma\rho} \frac{p^\mu p^\nu}{p^2} + \frac{4}{9} \delta^{\mu\nu} \delta^{\rho\sigma}, \end{aligned} \quad (\text{A12})$$

$$\mathcal{T}_3^{\mu\nu\rho\sigma}(p) \equiv \left(\frac{p^\mu p^\nu}{p^2} - \frac{\delta^{\mu\nu}}{3} \right) \left(\frac{p^\rho p^\sigma}{p^2} - \frac{\delta^{\rho\sigma}}{3} \right), \quad (\text{A13})$$

Subsequently, the inverse of the matrix \mathbf{W} is written as

$$\mathbf{\Gamma}^{\mu\nu\rho\sigma} \equiv \begin{pmatrix} \Gamma_{RR}^{(2)} & \Gamma_{RC}^{(2)} & \Gamma_{RS}^{(2)\rho\sigma} \\ \Gamma_{CR}^{(2)} & \Gamma_{CC}^{(2)} & \Gamma_{CS}^{(2)\rho\sigma} \\ \Gamma_{SR}^{(2)\mu\nu} & \Gamma_{SC}^{(2)\mu\nu} & \Gamma_{SS}^{(2)\mu\nu\rho\sigma} \end{pmatrix}, \quad (\text{A14})$$

and the following notation is introduced:

$$W_{ab}^{(2)} = g_{ab}, \quad \Gamma_{ab}^{(2)} = h_{ab}, \quad (\text{A15})$$

$$W_{cS}^{(2)\mu\nu} = \Delta^{\mu\nu} g_{cS}, \quad \Gamma_{cS}^{(2)\mu\nu} = \Delta^{\mu\nu} h_{cS}, \quad (\text{A16})$$

$$W_{SS}^{(2)\mu\nu\rho\sigma} = \sum_{i=1}^3 \mathcal{T}_i^{\mu\nu\rho\sigma} g_{SSi}, \quad \Gamma_{SS}^{(2)\mu\nu\rho\sigma} = \sum_{i=1}^3 \mathcal{T}_i^{\mu\nu\rho\sigma} h_{SSi}. \quad (\text{A17})$$

The h functions are related to the g functions by

$$h_{ab} = g_{ab}^{-1} - \frac{2}{3} g_{ac}^{-1} g_{cS} h_{bS}, \quad (\text{A18})$$

$$h_{aS} = \frac{3}{2} \frac{g_{bS} g_{ba}^{-1}}{(g_{cS} g_{cd}^{-1} g_{dS} + 5g_{SS1} - 4g_{SS2} - g_{SS3})}, \quad (\text{A19})$$

$$h_{SS1} = \frac{1}{4} g_{SS1}^{-1}, \quad (\text{A20})$$

$$h_{SS2} = \frac{g_{SS1}^{-1} g_{SS2}}{4(g_{SS2} - g_{SS1})}, \quad (\text{A21})$$

$$h_{SS3} = \frac{1}{2} \left(3g_{cS} h_{cS} + 32g_{SS1} h_{SS1} - 16g_{SS2} h_{SS1} \right. \\ \left. - 10g_{SS3} h_{SS1} - 16g_{SS1} h_{SS2} + 8g_{SS2} h_{SS2} + 8g_{SS3} h_{SS2} \right) \\ \times \frac{1}{5g_{SS1} - 4g_{SS2} - g_{SS3}}. \quad (\text{A22})$$

Hence, we have obtained $\Gamma^{(2)}$.

APPENDIX B: VERTICES

In this appendix, all vertices up to fourth order which appear in the FHA are given. First, the so called pure nematic vertices are discussed.

1. Nematic vertices

The pure nematic vertices are those involving correlation functions of the nematic order parameter $S_R^{\mu\nu}$. Clearly, these are $\gamma_{SS}^{(2)}$, $\gamma_{SSS}^{(3)}$, and $\gamma_{SSSS}^{(4)}$. For instance, the vertex $\gamma_{SS}^{(2)}$ can be obtained from $\Gamma_{SS}^{(2)\mu\nu\rho\sigma}$ as defined in the previous appendix.

In what follows, the limit $p \rightarrow 0$ is considered, with \vec{p} parallel to the orientational vector $\vec{\eta}$.² Consequently $\Delta^{\mu\nu} \rightarrow \mathcal{N}^{\mu\nu}$. Thus

$$\gamma_{SS}^{(2)}(0) = \mathcal{N}^{\mu\nu} \mathcal{N}^{\rho\sigma} \Gamma_{SS}^{(2)\mu\nu\rho\sigma}(0) \\ = \sum_{i=1}^3 h_{SSi} \mathcal{T}_i^{\mu\nu\rho\sigma} \mathcal{N}^{\mu\nu} \mathcal{N}^{\rho\sigma} = -\frac{20}{9} h_{SS1}(0) + \frac{16}{9} h_{SS2}(0) + \frac{4}{9} h_{SS3}(0)$$

²One can show that parallel alignment of \vec{p} and $\vec{\eta}$ has highest instability temperature [17]. In other words close to the spinodal, the angle θ between \vec{p} and $\vec{\eta}$ is zero.

$$= -\lim_{p \rightarrow 0} \frac{1}{(g_{CS}(p)g_{CD}^{-1}(p)g_{DS}(p) + 5g_{SS1}(p) - 4g_{SS2}(p) - g_{SS3}(p))} = \frac{5}{f_R^2}. \quad (\text{B1})$$

The three-point nematic vertex is

$$\begin{aligned} \gamma_{SSS}^{(3)}(0, 0) &= \mathcal{N}\mathcal{N}\mathcal{N}\Gamma_{SSS}^{(3)}(0, 0) = -[\mathcal{N}\Gamma_{SS}^{(2)}(0)]^3 W_{SSS}^{(3)}(0, 0) \\ &= -\left[\frac{15}{2f_R^2}\right]^3 \mathcal{N}\mathcal{N}\mathcal{N}W_{SSS}^{(3)}(0, 0) \\ &= -\left[\frac{15}{2f_R^2}\right]^3 f_R^3 \left(\frac{2}{3}\right)^3 \frac{2}{35} = -\frac{1}{f_R^3} \frac{50}{7}, \end{aligned} \quad (\text{B2})$$

where we have used the identities

$$\mathcal{N}^{\mu\nu}\Gamma_{SS}^{(2)\mu\nu\rho\sigma}(0) = \lim_{p \rightarrow 0} \sum_{i=1}^3 h_{SSi}(p) \mathcal{T}_i^{\mu\nu\rho\sigma}(p) \mathcal{N}^{\mu\nu} = \frac{15}{2f_R^2} \mathcal{N}^{\rho\sigma}, \quad (\text{B3})$$

and

$$\begin{aligned} \mathcal{N}^{\mu\nu}\mathcal{N}^{\rho\sigma}\mathcal{N}^{\kappa\lambda}W_{SSS}^{(3)\mu\nu\rho\sigma\kappa\lambda}(0, 0) &= f_R^3(2/3)^3 \langle [P_2(\cos\theta)]^3 \rangle_0 \\ &= f_R^3(2/3)^3 \int_{-1}^1 dx [P_2(x)]^3 / 2 = f_R^3(2/3)^3 (2/35). \end{aligned} \quad (\text{B4})$$

Subsequently, the four-point nematic vertex function can be computed,

$$\begin{aligned} \gamma_{SSSS}^{(4)}(0, 0, 0) &= \mathcal{N}\mathcal{N}\mathcal{N}\mathcal{N}\Gamma_{SSSS}^{(4)}(0, 0, 0) \\ &= -[\mathcal{N}\Gamma_{SS}^{(2)}(0)]^4 W_{SSSS}^{(4)}(0, 0, 0) \\ &\quad + 3[\mathcal{N}\Gamma_{SS}^{(2)}(0)]^4 W_{SSS}^{(3)}(0, 0) \Gamma_{SS}^{(2)}(0) W_{SSS}^{(3)}(0, 0) \\ &\quad + 3[\mathcal{N}\Gamma_{SS}^{(2)}(0)]^4 W_{SS}^{(2)}(0) W_{SS}^{(2)}(0) \\ &= \frac{1}{f_R^4} \frac{2550}{49}, \end{aligned} \quad (\text{B5})$$

where we have used that

$$\mathcal{N}\mathcal{N}\mathcal{N}\mathcal{N}W_{SSSS}^{(4)}(0, 0, 0) = f_R^4(2/3)^4 \langle [P_2(\cos\theta)]^4 \rangle = f_R^4(2/3)^4 (3/35), \quad (\text{B6})$$

$$\mathcal{N}\mathcal{N}W_{SSS}^{(3)}(0, 0) = f_R^3(2/3)^2 (2/35) \mathcal{N}, \quad (\text{B7})$$

$$\mathcal{N}\mathcal{N}W_{SS}^{(2)}(0) = f_R^2(2/3)^2 (1/5). \quad (\text{B8})$$

2. Density coefficients

Now the expressions for the pure density vertices are listed. The coefficient $\gamma_{\psi\psi}^{(2)}$ is given by

$$\gamma_{\psi\psi}^{(2)}(Q) = \epsilon_a \epsilon_b \Gamma_{ab}^{(2)}(Q) = h_{RR}(Q) + h_{RR}(Q) - 2h_{RC}(Q), \quad (\text{B9})$$

where the Roman indices a, b sum over R, C . At this point, we introduce the shorthand notation

$$\gamma_{ab} = \Gamma_{ab}^{(2)}(Q). \quad (\text{B10})$$

The coefficient $\gamma_{\psi\psi\psi}^{(3)}$ is

$$\begin{aligned} \gamma_{\psi\psi\psi}^{(3)}(Q_1, Q_2) &= \epsilon_a \epsilon_b \epsilon_c \Gamma_{abc}^{(3)}(Q_1, Q_2) \\ &= -z_a(Q_1) z_b(Q_2) z_c(-Q_1 - Q_2) W_{abc}^{(3)}(Q_1, Q_2) \end{aligned} \quad (\text{B11})$$

with $|Q_1| = |Q_2| = |Q_1 + Q_2|$ (thus $\hat{Q}_1 \cdot \hat{Q}_2 = -1/2$) and where

$$z_a(Q) \equiv \epsilon_{a'} \Gamma_{a'a}^{(2)}(Q), \quad (\text{B12})$$

hence

$$z_R(Q) = h_{RR}(Q) - h_{RC}(Q), \quad z_C(Q) = h_{RC}(Q) - h_{CC}(Q). \quad (\text{B13})$$

The three point single chain correlation functions are (again with $\hat{Q}_1 \cdot \hat{Q}_2 = -1/2$)

$$W_{RRR}^{(3)}(Q_1, Q_2) = w_{RRR}, \quad w_{RRR} = f_R^3 K_{R1}^{(3)}(y, -1/2), \quad (\text{B14})$$

$$W_{RRC}^{(3)}(Q_1, Q_2) = w_{RRC}, \quad w_{RRC} = f_R^2 f_C K_C^{(1)}(x) K_{R2}^{(2)}(y, -1/2), \quad (\text{B15})$$

$$W_{RCC}^{(3)}(Q_1, Q_2) = w_{RCC}, \quad w_{RCC} = f_R f_C^2 K_{C2}^{(2)}(x, -1/2) K_R^{(1)}(y), \quad (\text{B16})$$

$$W_{CCC}^{(3)}(Q_1, Q_2) = w_{CCC}, \quad w_{CCC} = f_C^3 K_{C1}^{(3)}(x, -1/2), \quad (\text{B17})$$

where $w_{RRC} = w_{RCR} = w_{CRR}$ and $w_{RCC} = w_{CCR} = w_{CRC}$. Again the K function are given in Appendix C.

The coefficient $\gamma_{\psi\psi\psi\psi}^{(4)}$ is (with $|Q_1| = |Q_2| = |Q_3| = |Q_1 + Q_2 + Q_3|$)

$$\begin{aligned} \gamma_{\psi\psi\psi\psi}^{(4)}(Q_1, Q_2, Q_3) &= \epsilon_a \epsilon_b \epsilon_c \epsilon_d \Gamma_{abcd}^{(4)}(Q_1, Q_2, Q_3) \\ &= M_1(Q_1, Q_2, Q_3) + M_2(Q_1, Q_2, Q_3) \end{aligned} \quad (\text{B18})$$

where

$$M_1(Q_1, Q_2, Q_3) = -z_a(Q_1) z_b(Q_2) z_c(Q_3) z_d(-Q_1 - Q_2 - Q_3) W_{abcd}^{(4)}(Q_1, Q_2, Q_3), \quad (\text{B19})$$

$$\begin{aligned} M_2(Q_1, Q_2, Q_3) &= z_a(Q_1) z_b(Q_2) z_c(Q_3) z_d(-Q_1 - Q_2 - Q_3) \\ &\times \left[W_{abe}^{(3)}(Q_1, Q_2) \Gamma_{ef}^{(2)}(-Q_1 - Q_2) W_{fcd}^{(3)}(Q_1 + Q_2, Q_3) \right. \\ &+ W_{ace}^{(3)}(Q_1, Q_3) \Gamma_{ef}^{(2)}(-Q_1 - Q_3) W_{fbd}^{(3)}(Q_1 + Q_3, Q_2) \\ &+ W_{ade}^{(3)}(Q_1, -Q_1 - Q_2 - Q_3) \Gamma_{ef}^{(2)}(Q_2 + Q_3) W_{fcb}^{(3)}(-Q_2 - Q_3, Q_3) \\ &+ \delta_K(Q_1 + Q_2) W_{ab}^{(2)}(Q_1) W_{cd}^{(2)}(Q_3) + \delta_K(Q_1 + Q_3) W_{ac}^{(2)}(Q_1) W_{bd}^{(2)}(Q_2) \\ &\left. + \delta_K(Q_2 + Q_3) W_{ad}^{(2)}(Q_1) W_{bc}^{(2)}(Q_2) \right]. \end{aligned} \quad (\text{B20})$$

Parts of the form

$$z_a z_b z_c z_d W_{abS}^{(3)} \Gamma_{SS}^{(2)} W_{cdS}^{(3)}, \quad (\text{B21})$$

though formerly present in Eq. (20), are not included in Eq. (B20), since these parts can be shown to be negligible with respect to the other terms comprising the four point density vertex.

We can compute the four-point single chain correlation functions. Their contribution is decomposed as

$$W_{RRRR}^{(4)}(Q_1, Q_2, Q_3) = f_R^4 K_R^{(4)}(y, c_1, c_2), \quad y = \ell q^*, \quad (\text{B22})$$

$$W_{CRRR}^{(4)}(Q_1, Q_2, Q_3) = f_C f_R^3 K_C^{(1)}(x) K_{R2}^{(3)}(y, c_1, c_2), \quad (\text{B23})$$

$$W_{CCRR}^{(4)}(Q_1, Q_2, Q_3) = f_C^2 f_R^2 K_{C2}^{(2)}(x, c_1) K_{R2}^{(2)}(y, c_1), \quad (\text{B24})$$

$$W_{CCCR}^{(4)}(Q_1, Q_2, Q_3) = f_C^3 f_R K_{C2}^{(3)}(x, c_1, c_2) K_R^{(1)}(y), \quad (\text{B25})$$

$$W_{CCCC}^{(4)}(Q_1, Q_2, Q_3) = f_C^4 K_C^{(4)}(x, c_1, c_2), \quad (\text{B26})$$

where

$$c_1 \equiv \frac{Q_1 \cdot Q_2}{|Q|^2}, \quad c_2 \equiv \frac{Q_1 \cdot Q_3}{|Q|^2}, \quad c_3 \equiv \frac{Q_2 \cdot Q_3}{|Q|^2} = -1 - c_1 - c_2. \quad (\text{B27})$$

Also, we have (with $c = Q_1 \cdot Q_2 / |Q|^2$)

$$W_{RRR}^{(3)}(Q_1, Q_2) = f_R^3 K_{R1}^{(3)}(y, c), \quad (\text{B28})$$

$$W_{RRC}^{(3)}(Q_1, Q_2) = f_R^2 f_C K_C^{(1)}(x(2+2c)) K_{R2}^{(2)}(y, c), \quad (\text{B29})$$

$$W_{RCR}^{(3)}(Q_1, Q_2) = f_R^2 f_C K_C^{(1)}(x) K_{R3}^{(2)}(y, c), \quad (\text{B30})$$

$$W_{CRR}^{(3)}(Q_1, Q_2) = f_R^2 f_C K_C^{(1)}(x) K_{R3}^{(2)}(y, c), \quad (\text{B31})$$

$$W_{RCC}^{(3)}(Q_1, Q_2) = f_R f_C^2 K_{C3}^{(2)}(x, c) K_R^{(1)}(y), \quad (\text{B32})$$

$$W_{CRC}^{(3)}(Q_1, Q_2) = f_R f_C^2 K_{C3}^{(2)}(x, c) K_R^{(1)}(y), \quad (\text{B33})$$

$$W_{CCR}^{(3)}(Q_1, Q_2) = f_R f_C^2 K_{C2}^{(2)}(x, c) K_R^{(1)}(y\sqrt{2+2c}), \quad (\text{B34})$$

$$W_{CCC}^{(3)}(Q_1, Q_2) = f_C^3 K_{C1}^{(3)}(x, c). \quad (\text{B35})$$

For the three morphologies it is sufficient to consider four particular configurations of “four vectors adding up to zero” for $\gamma_{\psi\psi\psi\psi}^{(4)}(Q_1, Q_2, Q_3)$. These configurations are, using Eqs. (B27),

$$c_1 = -1, \quad c_2 = -1, \quad c_3 = 1 \quad \longrightarrow \quad \gamma_{\psi\psi\psi\psi 1}^{(4)}, \quad (\text{B36})$$

$$c_1 = -1, \quad c_2 = -1/2, \quad c_3 = 1/2 \quad \longrightarrow \quad \gamma_{\psi\psi\psi\psi 2}^{(4)}, \quad (\text{B37})$$

$$c_1 = -1, \quad c_2 = 0, \quad c_3 = 0 \quad \longrightarrow \quad \gamma_{\psi\psi\psi\psi 3}^{(4)}, \quad (\text{B38})$$

$$c_1 = -1/2, \quad c_2 = -1/2, \quad c_3 = 0 \quad \longrightarrow \quad \gamma_{\psi\psi\psi\psi 4}^{(4)}, \quad (\text{B39})$$

where $\gamma_{\psi\psi\psi\psi i}^{(4)} \equiv \gamma_{\psi\psi\psi\psi}^{(4)}(Q_1, Q_2, Q_3)$.

3. Mixed vertices or coupling terms

The most interesting vertices are those involving both nematic as well as density order parameters, since these will give rise to coupling between nematic ordering and microphase ordering.

The coupling vertex $\gamma_{\psi\psi S}^{(3)}$ is

$$\begin{aligned}
\gamma_{\psi\psi S}^{(3)}(Q, -Q) &= \epsilon_a \epsilon_b \mathcal{N} \Gamma_{abS}^{(3)}(Q, -Q) \\
&= -z_a(Q) z_b(Q) \mathcal{N} \Gamma_{SS}^{(2)}(0) W_{abS}^{(3)}(Q, -Q) \\
&= -z_a(Q) z_b(Q) \mathcal{N} \Gamma_{SS}^{(2)}(0) \mathcal{N} \mathcal{N}(3/2) W_{abS}^{(3)}(Q, -Q) \\
&= -\frac{2}{3} z_a(Q) z_b(Q) z_S \bar{W}_{abS}^{(3)}(Q, -Q),
\end{aligned} \tag{B40}$$

where we have defined

$$z_S \mathcal{N}^{\mu\nu} \mathcal{N}^{\rho\lambda} \equiv \Gamma_{SS}^{(2)\mu\nu\rho\lambda}(0) \implies z_S = \frac{45}{4f_R^2}, \tag{B41}$$

and

$$\bar{W}_{abS}^{(3)}(Q, -Q) = \mathcal{N} W_{abS}^{(3)}(Q, -Q). \tag{B42}$$

It is straightforward to show that

$$W_{RRS}^{(3)\mu\nu}(Q, -Q) = f_R W_{RS}^{(2)\mu\nu}(Q), \tag{B43}$$

$$W_{RCS}^{(3)\mu\nu}(Q, -Q) = f_R W_{CS}^{(2)\mu\nu}(Q), \tag{B44}$$

$$W_{CCS}^{(3)\mu\nu}(Q, -Q) = 0. \tag{B45}$$

Hence

$$\bar{W}_{RRS}^{(3)}(Q, -Q) = w_{RRS} P_2(\hat{Q} \cdot \eta), \quad w_{RRS} = \frac{2}{3} f_R^3 K_{RS}^{(2)}(y), \tag{B46}$$

$$\bar{W}_{RCS}^{(3)}(Q, -Q) = w_{RCS} P_2(\hat{Q} \cdot \eta), \quad w_{RCS} = \frac{2}{3} f_R^2 f_C K_C^{(1)}(x) K_{S0}^{(1)}(y), \tag{B47}$$

$$W_{CCS}^{(3)\mu\nu}(Q, -Q) = 0, \quad w_{CCS} = 0, \tag{B48}$$

where $w_{RCS} = w_{CRS}$.

The four-point vertex $\gamma_{\psi\psi SS}^{(4)}$ reads

$$\begin{aligned}
\gamma_{\psi\psi SS}^{(4)}(Q, -Q, 0) &= \epsilon_a \epsilon_b \mathcal{N} \mathcal{N} \Gamma_{abSS}^{(4)}(Q, -Q, 0) \\
&= -\left(\frac{2}{3}\right)^2 z_a(Q) z_b(Q) z_S^2 \left[\bar{W}_{abSS}^{(4)}(Q, -Q, 0) - \bar{W}_{SS}^{(2)}(0) W_{ab}^{(2)}(Q) \right. \\
&\quad \left. - z_S \bar{W}_{abS}^{(3)}(Q, -Q) \bar{W}_{SSS}^{(3)}(0, 0) - 2 \bar{W}_{aS_c}^{(3)}(Q, 0) \Gamma_{cd}^{(2)}(Q) \bar{W}_{dbS}^{(3)}(Q, -Q) \right],
\end{aligned} \tag{B49}$$

with

$$\bar{W}_{abSS}^{(4)}(Q, -Q, 0) = \mathcal{N}\mathcal{N}W_{abSS}^{(4)}(Q, -Q, 0), \quad (\text{B50})$$

$$\bar{W}_{SS}^{(2)}(0) = \mathcal{N}\mathcal{N}W_{SS}^{(2)}(0), \quad (\text{B51})$$

$$\bar{W}_{abS}^{(3)}(Q, -Q) = \mathcal{N}W_{abS}^{(3)}(Q, -Q). \quad (\text{B52})$$

For instance, $W_{RRSS}^{(4)}$ is

$$\bar{W}_{RRSS}^{(4)}(Q, -Q) = f_R^2 W_{SS}^{(2)\mu\nu\rho\sigma}(Q) \mathcal{N}^{\mu\nu} \mathcal{N}^{\rho\sigma} = f_R^4 \sum_{i=1}^3 K_{Si}^{(2)}(y) \mathcal{N}\mathcal{N}\mathcal{T}_i(Q), \quad (\text{B53})$$

and

$$\mathcal{T}_1^{\mu\nu\rho\lambda}(Q) \mathcal{N}^{\mu\nu} \mathcal{N}^{\rho\lambda} = -\frac{16}{9} P_2(\hat{Q} \cdot \eta) - \frac{4}{9}, \quad (\text{B54})$$

$$\mathcal{T}_2^{\mu\nu\rho\lambda}(Q) \mathcal{N}^{\mu\nu} \mathcal{N}^{\rho\lambda} = \frac{8}{9} P_2(\hat{Q} \cdot \eta) + \frac{8}{9}, \quad (\text{B55})$$

$$\mathcal{T}_3^{\mu\nu\rho\lambda}(Q) \mathcal{N}^{\mu\nu} \mathcal{N}^{\rho\lambda} = \frac{4}{9} [P_2(\hat{Q} \cdot \eta)]^2. \quad (\text{B56})$$

Thus

$$\bar{W}_{RRSS}^{(4)}(Q, -Q) = w_{RRSS0} + w_{RRSS1} P_2(\hat{Q} \cdot \eta) + w_{RRSS2} P_2^2(\hat{Q} \cdot \eta), \quad (\text{B57})$$

$$w_{RRSS0} = f_R^4 \left(\frac{2}{3}\right)^2 \left(-K_{S1}^{(2)}(y) + 2K_{S2}^{(2)}(y)\right), \quad (\text{B58})$$

$$w_{RRSS1} = f_R^4 \left(\frac{2}{3}\right)^2 \left(-4K_{S1}^{(2)}(y) + 2K_{S2}^{(2)}(y)\right), \quad (\text{B59})$$

$$w_{RRSS2} = f_R^4 \left(\frac{2}{3}\right)^2 K_{S3}^{(2)}(y). \quad (\text{B60})$$

Also

$$\begin{aligned} \bar{W}_{RCSS}^{(4)}(Q, -Q) &= f_R^3 f_C K_C^{(1)}(x) \sum_{i=1}^3 K_{Si}^{(1)}(y) \mathcal{N}\mathcal{N}\mathcal{T}_i(Q) \\ &= w_{RCSS0} + w_{RCSS1} P_2(\hat{Q} \cdot \eta) + w_{RCSS2} P_2^2(\hat{Q} \cdot \eta), \end{aligned} \quad (\text{B61})$$

$$w_{RCSS0} = f_C f_R^3 K_C^{(1)}(x) \left(\frac{2}{3}\right)^2 \left(-K_{S1}^{(1)}(y) + 2K_{S2}^{(1)}(y)\right), \quad (\text{B62})$$

$$w_{RCSS1} = f_C f_R^3 K_C^{(1)}(x) \left(\frac{2}{3}\right)^2 \left(-4K_{S1}^{(1)}(y) + 2K_{S2}^{(1)}(y)\right), \quad (\text{B63})$$

$$w_{RCSS2} = f_C f_R^3 K_C^{(1)}(x) \left(\frac{2}{3}\right)^2 K_{S3}^{(1)}(y). \quad (\text{B64})$$

and,

$$\bar{W}_{CCSS}^{(4)}(Q, -Q) = f_R^2 f_C^2 K_{C1}^{(2)}(x) \frac{4}{45} = w_{CCSS0}. \quad (\text{B65})$$

The three-point single chain correlation parts of Eq. (B49) can be obtained from Eqs. (B46)-(B48) and Eq. (B7).

Subsequently the $\gamma_{\psi\psi SS}^{(4)}$ vertex is decomposed in the following way,

$$\gamma_{\psi\psi SS}^{(4)}(Q, -Q, 0) = \gamma_{\psi\psi SS0}^{(4)} + \gamma_{\psi\psi SS1}^{(4)} P_2(\hat{Q} \cdot \eta) + \gamma_{\psi\psi SS2}^{(4)} P_2^2(\hat{Q} \cdot \eta), \quad (\text{B66})$$

where

$$\begin{aligned} \gamma_{\psi\psi SS0}^{(4)} = & - \left(\frac{2}{3}\right)^2 z_S^2 \left[z_R^2 w_{RRSS0} + 2z_R z_C w_{RCSS0} + z_C^2 w_{CCSS0} \right. \\ & \left. - w_{SS}(z_R^2 w_{RR} + 2z_R z_C w_{RC} + z_C^2 w_{CC}) \right], \end{aligned} \quad (\text{B67})$$

$$\begin{aligned} \gamma_{\psi\psi SS1}^{(4)} = & - \left(\frac{2}{3}\right)^2 z_S^2 \left[z_R^2 w_{RRSS1} + 2z_R z_C w_{RCSS1} \right. \\ & \left. - z_S(z_R^2 w_{RRS} + 2z_R z_C w_{RCS}) w_{SSS} \right], \end{aligned} \quad (\text{B68})$$

$$\begin{aligned} \gamma_{\psi\psi SS2}^{(4)} = & - \left(\frac{2}{3}\right)^2 z_S^2 \left[z_R^2 w_{RRSS2} + 2z_R z_C w_{RCSS2} \right. \\ & \left. - 2z_a z_b w_{acS} \gamma_{cd} w_{dbS} \right]. \end{aligned} \quad (\text{B69})$$

Finally, we have the four-point vertex function $\gamma_{\psi\psi\psi S}^{(4)}$

$$\begin{aligned} \gamma_{\psi\psi\psi S}^{(4)}(Q_1, Q_2, Q_3) = & \epsilon_a \epsilon_b \epsilon_c \mathcal{N} \Gamma_{abcS}^{(4)}(Q_1, Q_2, Q_3) \\ = & -\frac{2}{3} z_a(Q_1) z_b(Q_2) z_c(Q_3) z_S \\ & \times \left[\bar{W}_{abcS}^{(4)}(Q_1, Q_2, Q_3) \right. \\ & - W_{abe}^{(3)}(Q_1, Q_2) \Gamma_{ef}^{(2)}(Q_3) \bar{W}_{fcS}^{(3)}(-Q_3, Q_3) \\ & - W_{ace}^{(3)}(Q_1, Q_3) \Gamma_{ef}^{(2)}(Q_2) \bar{W}_{fbS}^{(3)}(-Q_2, Q_2) \\ & \left. - \bar{W}_{aSe}^{(3)}(Q_1, 0) \Gamma_{ef}^{(2)}(-Q_1) W_{fcb}^{(3)}(Q_1, Q_3) \right], \end{aligned} \quad (\text{B70})$$

with $Q_3 = -Q_1 - Q_2$. In the FHA, the terms $W_{AB}^{(2)} W_{CS}^{(2)}$ vanish.

It can be shown that the correlation function $\bar{W}_{RRRS}^{(4)}$ is

$$\bar{W}_{RRRS}^{(4)}(Q_1, Q_2, Q_3) = w_{RRRS} \left[P_2(\hat{Q}_1 \cdot \eta) + P_2(\hat{Q}_2 \cdot \eta) + P_2(\hat{Q}_3 \cdot \eta) \right], \quad (\text{B71})$$

$$w_{RRRS} = \frac{2}{3} f_R^4 K_S^{(3)}(y), \quad (\text{B72})$$

and

$$\begin{aligned} \bar{W}_{CRRS}^{(4)}(Q_1, Q_2, Q_3) + \bar{W}_{RCRS}^{(4)}(Q_1, Q_2, Q_3) + \bar{W}_{RRCS}^{(4)}(Q_1, Q_2, Q_3) = & w_{RRCS} \\ & \times \left[P_2(\hat{Q}_1 \cdot \eta) + P_2(\hat{Q}_2 \cdot \eta) + P_2(\hat{Q}_3 \cdot \eta) \right], \end{aligned} \quad (\text{B73})$$

$$w_{RRCS} = \frac{2}{3} f_R^3 f_C K_C^{(1)}(x) K_{CS}^{(2)}(y). \quad (\text{B74})$$

The correlation function $\bar{W}_{CCRS}^{(4)}$ is (with $Q_3 = -Q_1 - Q_2$)

$$\begin{aligned} \bar{W}_{CCRS}^{(4)}(Q_1, Q_2, Q_3) + \bar{W}_{CRCS}^{(4)}(Q_1, Q_2, Q_3) + \bar{W}_{RCCS}^{(4)}(Q_1, Q_2, Q_3) = w_{CCRS} \\ \times \left[P_2(\hat{Q}_1 \cdot \eta) + P_2(\hat{Q}_2 \cdot \eta) + P_2(\hat{Q}_3 \cdot \eta) \right], \end{aligned} \quad (\text{B75})$$

$$w_{CCRS} = \frac{2}{3} f_R^2 f_C^2 K_{C2}^{(2)}(x) K_{S0}^{(1)}(y). \quad (\text{B76})$$

The correlation function $\bar{W}_{CCCS}^{(4)}$ vanishes in the FHA.

We can derive that, using Eq. (B71), (B73) and (B75), the four-point vertex (which is fully symmetric in its arguments) is

$$\gamma_{\psi\psi\psi S}^{(4)}(Q_1, Q_2, Q_3) = \sigma_{\psi\psi\psi S} \left[P_2(\hat{Q}_1 \cdot \eta) + P_2(\hat{Q}_2 \cdot \eta) + P_2(\hat{Q}_3 \cdot \eta) \right], \quad (\text{B77})$$

with $Q_3 = -Q_1 - Q_2$, and where,

$$\begin{aligned} \sigma_{\psi\psi\psi S} = -\frac{2}{3} z_S \left[z_R^3 w_{RRRS} + z_R^2 z_C w_{RRCS} + z_R z_C^2 w_{CCRS} \right] \\ + \frac{2}{3} z_S \sum_{a,b,c,d,e} z_a z_b z_c w_{abd} \gamma_{de} w_{ecS}, \end{aligned} \quad (\text{B78})$$

and $z_R = z_R(q^*)$, $z_C = z_C(q^*)$. Note that indices $a, b, c, d, e = R, C$.

APPENDIX C: DEFINITION OF COIL AND ROD FUNCTIONS

In this appendix, we list the so called coil and rod functions which appear in single chain correlation functions and vertices as given in the previous appendices. The superscript of such a K denotes the number of integrations or internal points involved. For most K functions an explicit expression can be given, however for certain rod functions the integral form is retained, since no analytical form could be obtained.

The coil functions are

$$K_C^{(1)}(x) = \frac{1}{x} \left[1 - e^{-x} \right], \quad (\text{C1})$$

$$K_{C1}^{(2)}(x) = f_D(x) = \frac{2}{x^2} \left[e^{-x} + x - 1 \right], \quad (\text{C2})$$

$$K_{C2}^{(2)}(x) = 2K_C^{(1)}(x) - K_{C1}^{(2)}(x), \quad (\text{C3})$$

and

$$\begin{aligned} K_{C2}^{(2)}(x, c) &= \int_0^1 d\tau_1 \int_0^1 d\tau_2 e^{-x(1+c)(2-\tau_1-\tau_2)+xc|\tau_1-\tau_2|} \\ &= \frac{e^{-2(1+c)x} + (1+2c) - 2(1+c)e^{-x}}{(1+3c+2c^2)x^2}, \quad c \neq -\frac{1}{2}, -1, \end{aligned} \quad (\text{C4})$$

$$K_{C1}^{(2)}(x) = K_{C2}^{(2)}(x, -1) = f_D(x), \quad (\text{C5})$$

$$K_{C2}^{(2)}(x) = K_{C2}^{(2)}(x, -1/2) = \frac{2}{x^2} \left[1 - (1+x)e^{-x} \right], \quad (\text{C6})$$

$$\begin{aligned}
K_{C_3}^{(2)}(x, c) &= \int_0^1 d\tau_1 \int_0^1 d\tau_2 e^{-x(1+c)|\tau_1-\tau_2|-x(1+c)(1-\tau_2)+xc(1-\tau_1)} \\
&= \frac{e^{-2(1+c)x} + (3 + 8c + 4c^2) - 2(1+c)(2+x+2c(1+x))e^{-x}}{2(1+c)(1+2c)x^2}, \tag{C7}
\end{aligned}$$

$$c \neq -\frac{1}{2}, -1,$$

$$K_{C_3}^{(2)}(x, -1/2) = \frac{2}{x^2} [1 - (1+x)e^{-x}], \quad K_{C_3}^{(2)}(x, -1) = \frac{1}{x} [1 - e^{-x}]. \tag{C8}$$

The coil functions involving three or four integrals are

$$K_{C_1}^{(3)}(x, c) = \int_0^1 d\tau_1 \int_0^1 d\tau_2 \int_0^1 d\tau_3 e^{-x(1+c)|\tau_1-\tau_3|-x(1+c)|\tau_2-\tau_3|+xc|\tau_1-\tau_2|}, \tag{C9}$$

$$K_{C_1}^{(3)}(x, -1/2) = \frac{6}{x^3} [x(1 + e^{-x}) - 2(1 - e^{-x})]. \tag{C10}$$

and

$$K_{C_2}^{(3)}(x, c_1, c_2) = \int_0^1 d\tau_1 \int_0^1 d\tau_2 \int_0^1 d\tau_3 e^{xc_3(1-\tau_1+|\tau_2-\tau_3|)+xc_2(1-\tau_2+|\tau_1-\tau_3|)+xc_1(1-\tau_3+|\tau_1-\tau_2|)}, \tag{C11}$$

$$\begin{aligned}
K_C^{(4)}(x, c_1, c_2) &= \int_0^1 d\tau_1 \int_0^1 d\tau_2 \int_0^1 d\tau_3 \int_0^1 d\tau_4 \\
&\times e^{xc_3(|\tau_1-\tau_4|+|\tau_2-\tau_3|)+xc_2(|\tau_2-\tau_4|+|\tau_1-\tau_3|)+xc_1(|\tau_3-\tau_4|+|\tau_1-\tau_2|)}, \tag{C12}
\end{aligned}$$

with $c_3 = -1 - c_1 - c_2$. Clearly explicit expressions for these integrals can be obtained, these are already given elsewhere.

The particular rod functions of interest are

$$K_R^{(1)}(y) = \frac{\text{Si}(y)}{y}, \tag{C13}$$

$$K_{R1}^{(2)}(y) = \frac{2}{y^2} [-1 + \cos y + y \text{Si}(y)], \tag{C14}$$

$$K_{R2}^{(2)}(y, c) = \int_0^1 ds_1 \int_0^1 ds_2 \frac{\sin y \sqrt{s_1^2 + s_2^2 + 2s_1s_2c}}{y \sqrt{s_1^2 + s_2^2 + 2s_1s_2c}}, \tag{C15}$$

$$K_{R3}^{(2)}(y, c) = \int_0^1 ds_1 \int_0^1 ds_2 \frac{\sin y \sqrt{s_1^2 + s_2^2(2+2c) - s_1s_2(2+2c)}}{y \sqrt{s_1^2 + s_2^2(2+2c) - s_1s_2(2+2c)}}, \tag{C16}$$

and

$$\begin{aligned}
K_{R1}^{(3)}(y, c) &= \int_0^1 ds_1 \int_0^1 ds_2 \int_0^1 ds_3 \frac{\sin y \sqrt{\tau_{R1}^{(3)}}}{y \sqrt{\tau_{R1}^{(3)}}}, \tag{C17} \\
\tau_{R1}^{(3)} &= (s_1 - s_3)^2 + 2(s_1 - s_3)(s_2 - s_3)c + (s_2 - s_3)^2,
\end{aligned}$$

$$\begin{aligned}
K_{R2}^{(3)}(y, c_1, c_2) &\equiv \int_0^1 ds_1 \int_0^1 ds_2 \int_0^1 ds_3 \frac{\sin y \sqrt{\tau_{R2}^{(3)}}}{y \sqrt{\tau_{R2}^{(3)}}}, \\
\tau_{R2}^{(3)} &= s_3^2 + (s_1 - s_3)^2 + (s_2 - s_3)^2 - 2s_3(s_1 - s_3)c_1 \\
&\quad - 2s_3(s_2 - s_3)c_2 - 2(s_1 - s_3)(s_2 - s_3)(1 + c_1 + c_2),
\end{aligned} \tag{C18}$$

$$\begin{aligned}
K_R^{(4)}(y, c_1, c_2) &\equiv \int_0^1 ds_1 \int_0^1 ds_2 \int_0^1 ds_3 \int_0^1 ds_4 \frac{\sin y \sqrt{\tau_R^{(4)}}}{y \sqrt{\tau_R^{(4)}}}, \\
\tau_R^{(4)} &= (s_1 - s_4)^2 + (s_2 - s_4)^2 + (s_3 - s_4)^2 + 2(s_1 - s_4)(s_2 - s_4)c_1 \\
&\quad + 2(s_1 - s_4)(s_3 - s_4)c_2 - 2(s_2 - s_4)(s_3 - s_4)(1 + c_1 + c_2).
\end{aligned} \tag{C19}$$

Also, there are the so called mixed terms

$$K_{RS}^{(2)}(y) = \frac{1}{y^3} [4y - y \cos y - 3 \sin y - y^2 \text{Si}(y)], \tag{C20}$$

$$\begin{aligned}
K_{CS}^{(2)}(y) &= \int_0^1 ds_1 \int_0^1 ds_2 \frac{s_2(2s_2 - s_1)}{\tau_{CS}^{(2)5} y^3} [(y^2 \tau_{CS}^{(2)2} - 3) \sin(y \tau_{CS}^{(2)}) + 3y \tau_{CS}^{(2)} \cos(y \tau_{CS}^{(2)})], \\
\tau_{CS}^{(2)} &= \sqrt{s_1^2 + s_2^2 - s_1 s_2}.
\end{aligned} \tag{C21}$$

Finally, we list the K function which appear as factors in vertices with nematic order parameters,

$$\begin{aligned}
K_{S0}^{(1)}(y) &\equiv \int_0^1 \frac{ds}{s^2} \left(-\frac{d^2}{dy^2} + \frac{1}{y} \frac{d}{dy} \right) \frac{\sin ys}{ys} \\
&= \left(-\frac{1}{2y^3} \right) [3y \cos y - 3 \sin y + y^2 \text{Si}(y)],
\end{aligned} \tag{C22}$$

$$\begin{aligned}
K_{S1}^{(1)}(y) &\equiv \int_0^1 \frac{ds}{s^4} \left(\frac{1}{y^2} \frac{d^2}{dy^2} - \frac{1}{y^3} \frac{d}{dy} \right) \frac{\sin ys}{ys} \\
&= \frac{1}{8y^5} [y^4 \text{Si}(y) + y(y^2 + 6) \cos y + (y^2 - 6) \sin y],
\end{aligned} \tag{C23}$$

$$\begin{aligned}
K_{S2}^{(1)}(y) &\equiv \int_0^1 \frac{ds}{s^4} \left(\frac{1}{y} \frac{d^3}{dy^3} - \frac{1}{y^2} \frac{d^2}{dy^2} + \frac{1}{y^3} \frac{d}{dy} \right) \frac{\sin ys}{ys} \\
&= \frac{1}{8y^5} [y^4 \text{Si}(y) + y(y^2 - 18) \cos y + (18 - 7y^2) \sin y],
\end{aligned} \tag{C24}$$

$$\begin{aligned}
K_{S3}^{(1)}(y) &\equiv \int_0^1 \frac{ds}{s^4} \left(\frac{d^4}{dy^4} - \frac{6}{y} \frac{d^3}{dy^3} + \frac{15}{y^2} \frac{d^2}{dy^2} - \frac{15}{y} \frac{d}{dy} \right) \frac{\sin ys}{ys} \\
&= \frac{1}{8y^5} [3y^3 \text{Si}(y) - 5y(y^2 - 42) \cos y + 15(5y^2 - 14) \sin y],
\end{aligned} \tag{C25}$$

and

$$K_{S1}^{(2)}(y) \equiv \int_0^1 \int_0^1 \frac{ds ds'}{(s - s')^4} \left(\frac{1}{y^2} \frac{d^2}{dy^2} - \frac{1}{y^3} \frac{d}{dy} \right) \frac{\sin y(s - s')}{y(s - s')}$$

$$= \left(\frac{1}{12y^5} \right) \left[3y^4 \text{Si}(y) - 8y^3 + 3y(y^2 - 2) \cos y + 3(y^2 + 2) \sin y \right], \quad (\text{C26})$$

$$\begin{aligned} K_{S^2}^{(2)}(y) &\equiv \int_0^1 \int_0^1 \frac{ds ds'}{(s-s')^4} \left(\frac{1}{y} \frac{d^3}{dy^3} - \frac{1}{y^2} \frac{d^2}{dy^2} + \frac{1}{y^3} \frac{d}{dy} \right) \frac{\sin y(s-s')}{y(s-s')} \\ &= \left(\frac{1}{4y^5} \right) \left[y^4 \text{Si}(y) + y(y^2 + 6) \cos y + (y^2 - 6) \sin y \right], \end{aligned} \quad (\text{C27})$$

$$\begin{aligned} K_{S^3}^{(2)}(y) &\equiv \int_0^1 \int_0^1 \frac{ds ds'}{(s-s')^4} \left(\frac{d^4}{dy^4} - \frac{6}{y} \frac{d^3}{dy^3} + \frac{15}{y^2} \frac{d^2}{dy^2} - \frac{15}{y} \frac{d}{dy} \right) \frac{\sin y(s-s')}{y(s-s')} \\ &= \left(\frac{1}{12y^5} \right) \left[9y^4 \text{Si}(y) - 64y^3 + y(9y^2 - 210) \cos y - 15(y^2 - 14) \sin y \right], \end{aligned} \quad (\text{C28})$$

and

$$\begin{aligned} K_S^{(3)}(y) &= \int_0^1 ds_1 \int_0^1 ds_2 \int_0^1 ds_3 \frac{(s_1 - s_3)(s_2 - s_3)}{\tau_S^{(3)5} y^3} \left[(y^2 \tau_S^{(3)2} - 3) \sin(y \tau_S^{(3)}) + 3y \tau_S^{(3)} \cos(y \tau_S^{(3)}) \right], \\ \tau_S^{(3)} &= \sqrt{s_1^2 + s_2^2 + s_3^2 - s_1 s_2 - s_1 s_3 - s_2 s_3}. \end{aligned} \quad (\text{C29})$$

REFERENCES

- [1] L. Leibler, *Macromolecules* **13**, 1602 (1980).
- [2] A. N. Semenov, *Sov. Phys. JETP* **61**, 733 (1985).
- [3] M. W. Matsen and M. Schick, *Phys. Rev. Lett.* **72**, 2660 (1994).
- [4] F. S. Bates and G. H. Fredrickson, *Annu. Rev. Phys. Chem.* **21**, 525 (1990).
- [5] L. H. Radzilowski and S. I. Stupp, *Macromolecules* **27**, 7747 (1994).
- [6] L. H. Radzilowski, B. O. Carragher, and S. I. Stupp, *Macromolecules* **30**, 2110 (1997).
- [7] M. Lee, B.-K. Cho, N.-K. Oh, and W.-C. Zin, *Macromolecules* **34**, 1987 (2001).
- [8] M. Lee, J.-W. Kim, I.-W. Hwang, Y.-R. Kim, N.-K. Oh, and W.-C. Zin, *Adv. Mater.* **13**, 1363 (2001).
- [9] A. Schneider, J.-J. Zanna, M. Yamada, H. Finkelmann, and R. Thomann, *Macromolecules of i.d.* **33**, 649 (2000).
- [10] J. T. Chen, E. L. Thomas, C. K. Ober, and G. Mao, *Science* **273**, 343 (1996).
- [11] M. Muthukumar, C. K. Ober, and E. L. Thomas, *Science* **277**, 1225 (1997).
- [12] Z. R. Wagner, T. K. Roenigk, and F. E. Goodson, *Macromolecules* **34**, 5740 (2001).
- [13] R. Peck F. Elias, S. M. Clarke and E. M. Terentjev, *Macromolecules* **33**, 2060 (2000).
- [14] B. de Boer, *Design, synthesis, morphology, and properties of semiconducting block copolymers for photonic applications*, PhD thesis, University of Groningen, 2001.
- [15] R. Holyst and M. Schick, *J. Chem. Phys.* **96**, 730 (1992).
- [16] A. J. Liu and G. H. Fredrickson, *Macromolecules* **26**, 2817 (1993).
- [17] C. Singh, M. Goulian, A. J. Liu, and G. H. Fredrickson, *Macromolecules* **27**, 2974 (1994).
- [18] R. Holyst and P. Oswald, *Macromol. Theory Simul.* **10**, 1 (2001); R. Holyst and T. A. Vilgis, *Macromol. Theory Simul.* **5**, 573 (1996).
- [19] G. H. Fredrickson and L. Leibler, *Macromolecules* **23**, 531 (1990).
- [20] R. Holyst and M. Schick, *J. Chem. Phys.* **96**, 721 (1992).
- [21] M. Hamm, G. Goldbeck-Wood, A. V. Zvelindovsky, G. J. A. Sevink, and J. G. E. M. Fraaije, *Macromolecules* **34**, 8378 (2001); *J. Chem. Phys.* **116**, 3152 (2002).
- [22] R. R. Netz and M. Schick, *Phys. Rev. Lett.* **77**, 302 (1996).
- [23] M. W. Matsen and C. Barrett, *J. Chem. Phys.* **109**, 4108 (1998).
- [24] E. Gurovich, *Phys. Rev. Lett.* **74**, 482 (1995).
- [25] A. N. Semenov and S.V. Vasilenko, *Sov. Phys. JETP* **63**, 70 (1986).
- [26] A. Halperin, *Europhys. Lett.* **10**, 549 (1989).
- [27] A. N. Semenov and A. V. Subbotin, *Sov. Phys. JETP* **74**, 660 (1992).
- [28] D. R. M. Williams and G. H. Fredrickson, *Macromolecules* **25**, 3561 (1992).
- [29] D. R. M. Williams and A. Halperin, *Phys. Rev. Lett.* **71**, 1557 (1993).
- [30] A. M. Lapeña, S. C. Glotzer, S. A. Langer, and A. J. Liu, *Phys. Rev.* **E60**, R29 (1999).
- [31] W. Li and D. Gersappe, *Macromolecules* **34**, 6783 (2001).
- [32] J. Fukuda and H. Yokoyama, *J. Chem. Phys.* **115**, 4930 (2001).
- [33] R. J. Nap, C. Kok, G. ten Brinke, and S. I. Kuchanov, *Eur. Phys. J.* **E4**, 515 (2001).
- [34] R. J. Nap and G. ten Brinke, *Macromolecules* **35**, 952 (2002); cond-mat/0103531.
- [35] P. M. Chaikin and T. C. Lubensky, *Principles of condensed matter physics*, Cambridge University Press, 1995.

FIGURES

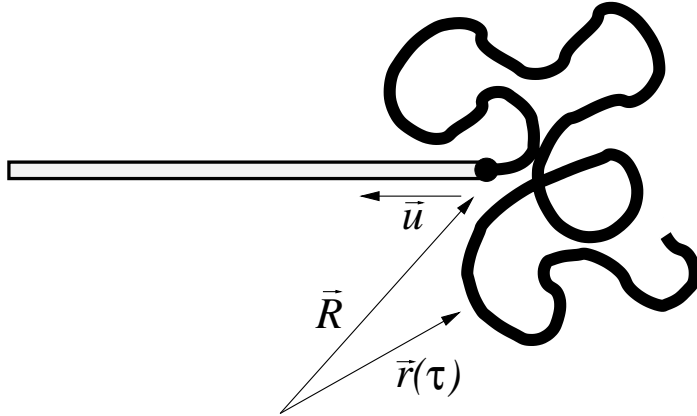


FIG. 1. Parametrization of the configuration of a rod-coil diblock.

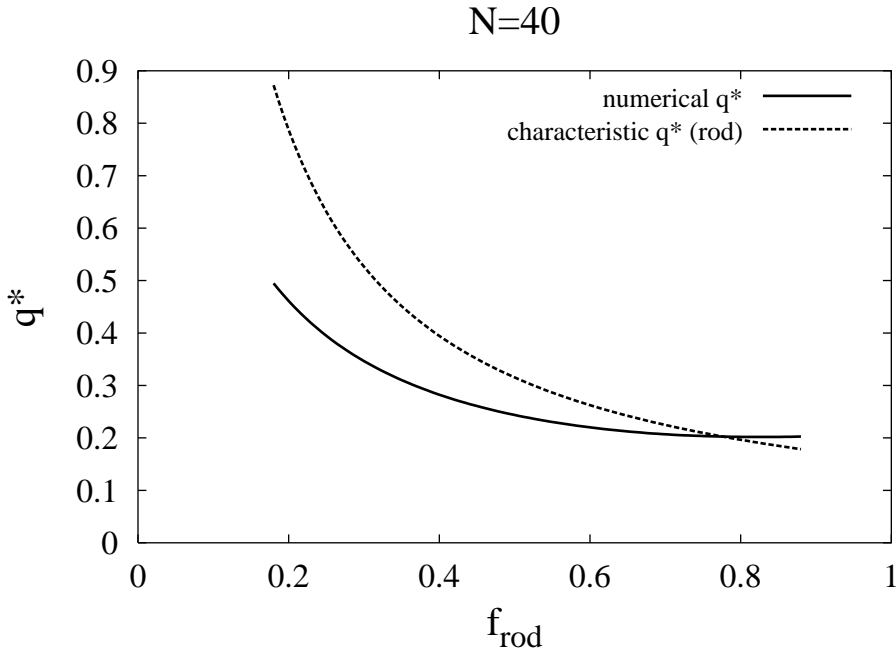


FIG. 2. The numerical value of the wave vector q^* for $N = 40$ as minimum of $\gamma_{\psi\psi}^{(2)}$ vs the characteristic rod wave vector $q^* = 2\pi/(Nf_R)$.

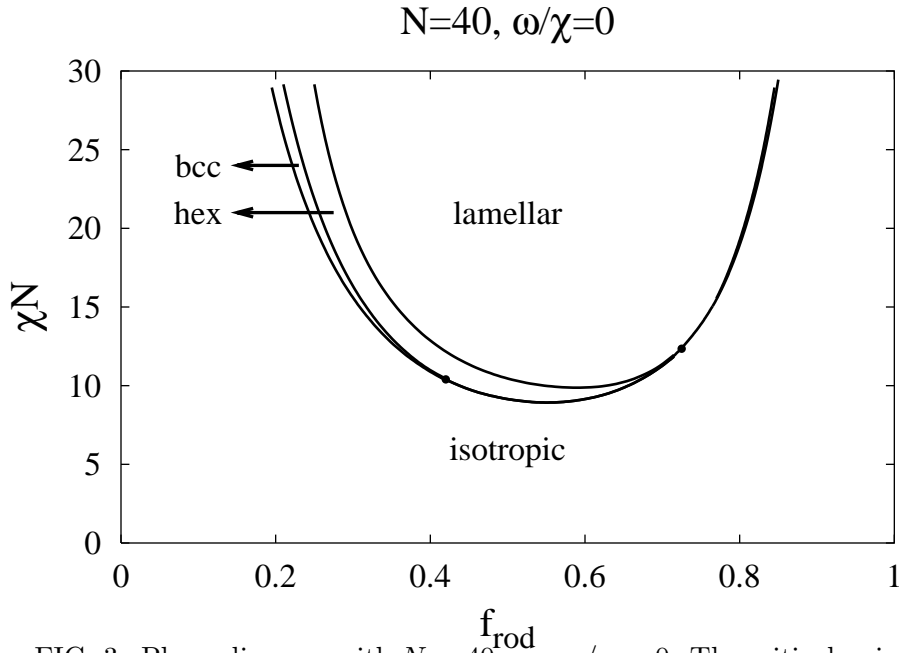


FIG. 3. Phase diagram with $N = 40, r = \omega/\chi = 0$. The critical point lies in the rod-rich region near $f_{rod} \simeq 0.73$ and there is a triple point near $f_{rod} \simeq 0.42$, separating the isotropic/BCC/HEX phases.

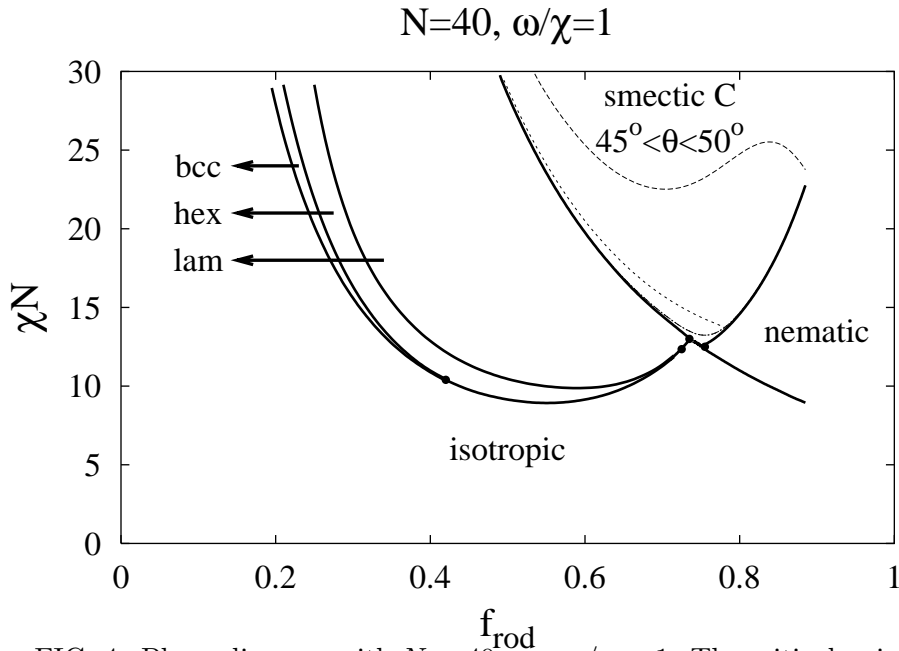


FIG. 4. Phase diagram with $N = 40, r = \omega/\chi = 1$. The critical point still lies near $f_{rod} \simeq 0.73$. The three other dots are triple points. The dashed curves in the smectic C phase are contour lines for the angle θ , separating intervals of 5° . The smallest value for θ is about 30° just at the phase boundaries near the triple points.

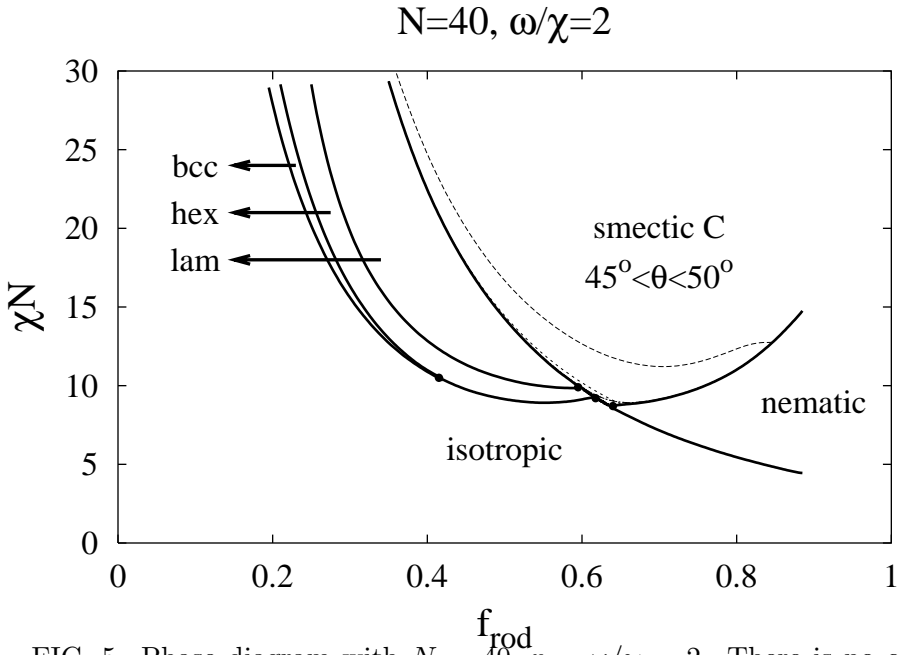


FIG. 5. Phase diagram with $N = 40$, $r = \omega/\chi = 2$. There is no critical point. All dots are triple points. The dashed curves in the smectic C phase are contour lines for the angle θ , separating intervals of 5° .

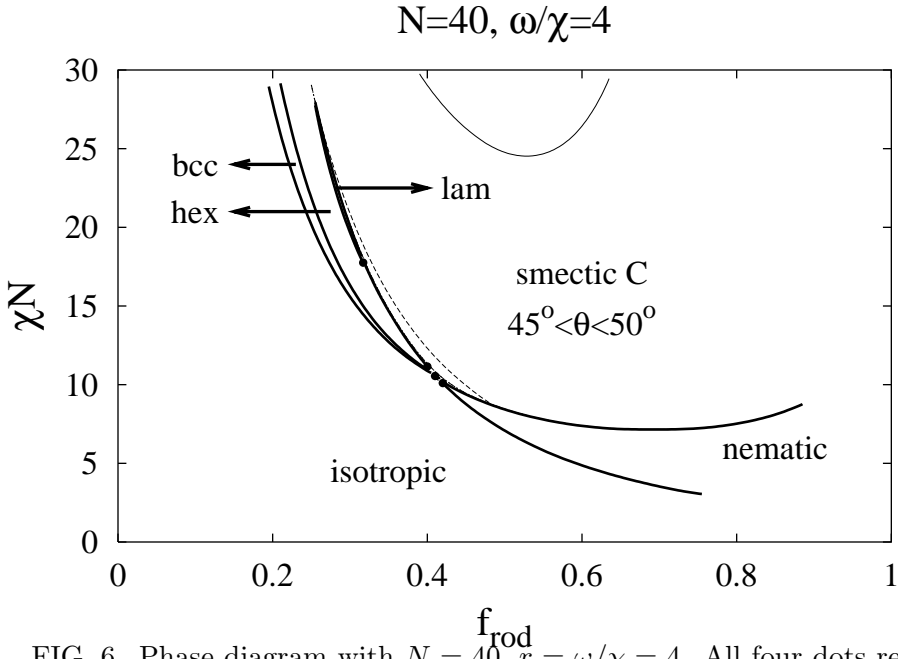


FIG. 6. Phase diagram with $N = 40$, $r = \omega/\chi = 4$. All four dots represent triple points. The dashed curves and the thin solid curve in the smectic C phase are contour lines for the angle θ , separating intervals of 5° .

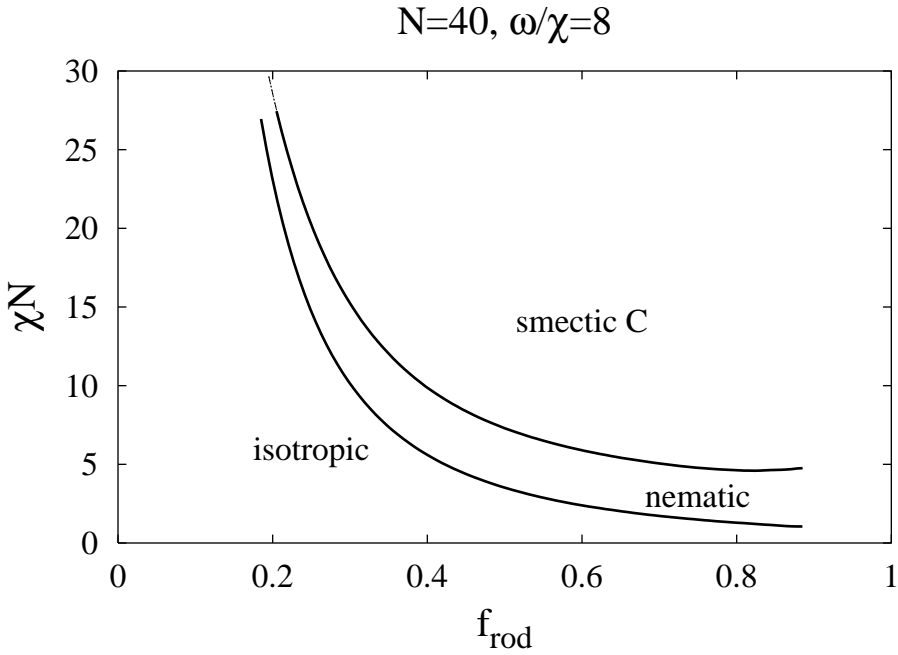


FIG. 7. Phase diagram with $N = 40, r = \omega/\chi = 8$. There are no triple points.

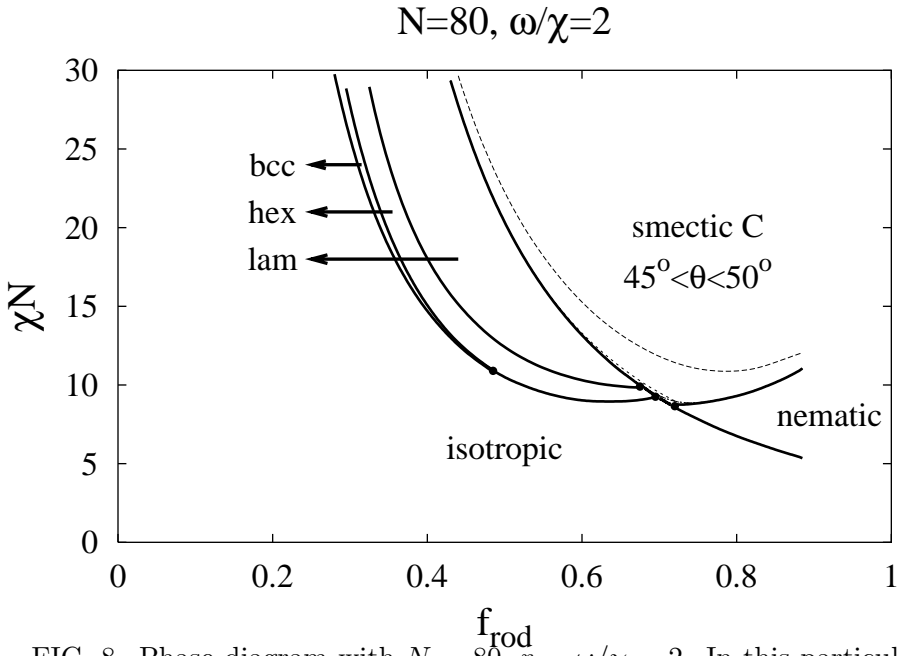


FIG. 8. Phase diagram with $N = 80, r = \omega/\chi = 2$. In this particular case there is no critical point and the dots are triple points. The dashed curves in the smectic C phase are contour lines for the angle θ , separating intervals of 5° .